# Isoform Diversity of Giant Proteins in Relation to Passive and Active Contractile Properties of Rabbit Skeletal Muscles

Lucas G. Prado,[1] Irina Makarenko,[2] Christian Andresen,[2] Martina Krüger,[2] Christiane A. Opitz,[1] and Wolfgang A. Linke[2]

[1]Institute of Physiology and Pathophysiology, University of Heidelberg, D-69120 Heidelberg, Germany
[2]Physiology and Biophysics Unit, University of Muenster, D-48149 Muenster, Germany

The active and passive contractile performance of skeletal muscle fibers largely depends on the myosin heavy chain (MHC) isoform and the stiffness of the titin spring, respectively. Open questions concern the relationship between titin-based stiffness and active contractile parameters, and titin's importance for total passive muscle stiffness. Here, a large set of adult rabbit muscles ($n = 37$) was studied for titin size diversity, passive mechanical properties, and possible correlations with the fiber/MHC composition. Titin isoform analyses showed sizes between ~3300 and 3700 kD; 31 muscles contained a single isoform, six muscles coexpressed two isoforms, including the psoas, where individual fibers expressed similar isoform ratios of 30:70 (3.4:3.3 MD). Gel electrophoresis and Western blotting of two other giant muscle proteins, nebulin and obscurin, demonstrated muscle type–dependent size differences of ≤70 kD. Single fiber and single myofibril mechanics performed on a subset of muscles showed inverse relationships between titin size and titin-borne tension. Force measurements on muscle strips suggested that titin-based stiffness is not correlated with total passive stiffness, which is largely determined also by extramyofibrillar structures, particularly collagen. Some muscles have low titin-based stiffness but high total passive stiffness, whereas the opposite is true for other muscles. Plots of titin size versus percentage of fiber type or MHC isoform (I-IIB-IIA-IID) determined by myofibrillar ATPase staining and gel electrophoresis revealed modest correlations with the type I fiber and MHC-I proportions. No relationships were found with the proportions of the different type II fiber/MHC-II subtypes. Titin-based stiffness decreased with the slow fiber/MHC percentage, whereas neither extramyofibrillar nor total passive stiffness depended on the fiber/MHC composition. In conclusion, a low correlation exists between the active and passive mechanical properties of skeletal muscle fibers. Slow muscles usually express long titin(s), predominantly fast muscles can express either short or long titin(s), giving rise to low titin-based stiffness in slow muscles and highly variable stiffness in fast muscles. Titin contributes substantially to total passive stiffness, but this contribution varies greatly among muscles.

The Journal of General Physiology

## INTRODUCTION

Textbook knowledge indicates that the type of myosin heavy chain (MHC) expressed in a skeletal muscle is a major determinant of that muscle's contractile characteristics. Slow MHC isoforms predominante in slow muscles, fast MHC isoforms in fast muscles (Staron and Pette, 1986). MHC is encoded by a multigene family consisting of several members expressed in a developmentally regulated and tissue-specific manner (Schiaffino and Reggiani, 1994). In adult mammalian muscles, four MHC isoforms have been identified, which are termed I (slow), IIA, IIX or IID, and IIB (all fast). The unique expression of any one of these MHC isoforms in a single muscle fiber is primarily responsible for the distinct fiber types observed in skeletal muscle after staining for myofibrillar ATPase following acid or alkaline preincubations (Termin et al., 1989). Both the myofibrillar ATPase activities and the MHC-based fiber type composition of a muscle can be used to predict the contractile properties of the whole muscle (Thomason et al., 1986; Ranatunga and Thomas, 1990). A close relationship has been suggested to exist between the isoforms of MHC and those of myosin light chains (Salviati et al., 1982; Schiaffino and Reggiani, 1994) and regulatory proteins in the sarcomere, e.g., the troponins (Salviati et al., 1982; Wade et al., 1990; O'Connell et al., 2004). Also the molecular compositions of both the sarcomeric M-band (Agarkova et al., 2004) and Z-disc (Sorimachi et al., 1997; MacArthur and North, 2004) correlate with muscle fiber type.

Titin (Wang et al., 1979), first described as connectin (Maruyama et al., 1976), is a giant protein in sarcomeres, which is expressed in different isoforms generated by alternative splicing from the transcript of a single titin gene (Labeit and Kolmerer, 1995). Titin molecules span across half sarcomeres and the I band segment acts as a molecular spring, whereas the A band part is

L.G. Prado and I. Makarenko contributed equally to this work.
Correspondence to Wolfgang A. Linke: wlinke@uni-muenster.de

Abbreviations used in this paper: BDM, 2,3-butanedione monoxime; MHC, myosin heavy chain; PT, passive tension; SL, sarcomere length.

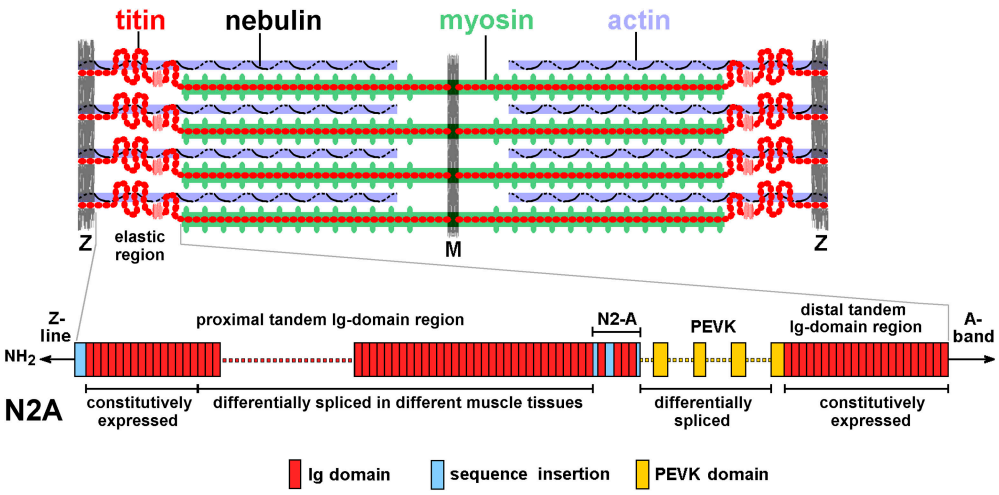


**Figure 1.** Titin and nebulin in the sarcomere and nomenclature of elastic I-band regions in the skeletal muscle titin isoforms, "N2A."

functionally stiff (Fig. 1). Titin's differentially spliced part is in the I band and in skeletal muscles expressing so-called "N2A-titin," there are two segments that vary in length in the different isoforms: a "proximal" tandem Ig region and the PEVK domain (Fig. 1). Titin has multiple roles in sarcomeric function (Neagoe et al., 2003; Granzier and Labeit, 2004; Miller et al., 2004; Tskhovrebova and Trinick, 2004) but is well recognized for being a main determinant of passive tension (PT) (Maruyama et al., 1984; Magid and Law, 1985; Horowits et al., 1986; Funatsu et al., 1990; Salviati et al., 1990). It has been shown that long titin isoforms give rise to relatively low PT, short titin isoforms to higher PT (Wang et al., 1991; Horowits, 1992; Linke et al., 1996; Granzier et al., 2000).

The largest titin sequenced to date (3,700 kD) is found in human soleus, a slow muscle with low myofibrillar PT (Trombitas et al., 1998), whereas small titin (3,400 kD) is expressed in the fast-twitch rabbit psoas (Freiburg et al., 2000), which has high myofibrillar PT (Linke et al., 1996). Many researchers have therefore assumed that the muscle type may be related to the titin size, in that fast muscles express short and stiff titin, slow muscles long and compliant titin. This idea, however, had never been tested, largely because of difficulties in resolving size differences of proteins in the MD range. We have recently optimized the detection of titin isoforms on 2% SDS-PAGE (Neagoe et al., 2002; Opitz et al., 2004). Here, by using sequenced titin isoforms as size markers, we determined the titin size variations in a set of 37 different adult rabbit skeletal muscles. Similarly, we analyzed the size distributions of two other giant muscle proteins: nebulin, an actin-binding protein acting as a thin filament length ruler (Kruger et al., 1991; Labeit et al., 1991); and obscurin, a sarcomere-associated signaling protein (Young et al., 2001) also suggested to provide an elastic link between adjacent myofibrils (Borisov et al., 2004). We find that isoform variability is low for nebulin (range, ~700–760 kD), modest for obscurin (~680–750 kD), but large for titin (3300–3700 kD). The titin size diversity is shown by single myofibril, single fiber, and fiber bundle mechanics to cause substantial differences in titin-based PT between muscles.

Two previously unresolved issues concern titin's importance for total passive muscle stiffness and the relationship between titin-based stiffness and active contractile parameters. Here we tested the hypothesis that titin-borne PT, adjustable by modifying the length of titin's elastic spring, is related to the active contractile properties characterized by the fiber/MHC composition. Fiber types I, IIA, and IIB/IID were discriminated by myosin ATPase staining, and MHC isoforms I, IIA, IIB, and IID were determined on SDS-PAGE. Only a low correlation with titin size and titin-based stiffness is found. Results suggest that predominantly slow muscles have long titin and low titin-borne PT, whereas fast muscles express long or short titin(s) and differ greatly in titin-based PT. Finally, we extend earlier evidence suggesting that a large contribution to a muscle's passive stiffness comes from extramyofibrillar structures, particularly collagen (Kovanen et al., 1984a; Gosselin et al., 1998; Ducomps et al., 2003). We demonstrate by fiber bundle mechanics that the relative contribution of titin versus that of the extracellular matrix to passive stiffness varies greatly among different muscles. Some muscles (e.g., soleus) have low titin-borne stiffness but high total passive stiffness, whereas the opposite is true for other muscles (e.g., psoas). Titin-based stiffness, but not extramyofibrillar stiffness, correlates with muscle type.

## MATERIALS AND METHODS

### Dissection of Rabbit Skeletal Muscles

Adult male New Zealand white rabbits (weight, 2–3 kg) obtained from the university's animal house were killed by the method of

captive bolt according to the recommendations of the institutional animal care committee (Medical Faculty, University of Heidelberg). Skeletal muscles were dissected with the help of a Rabbit Dissection Manual (Wingerd, 1985), and anatomical locations of skeletal muscles were verified using a rabbit anatomy atlas (Popesko et al., 1992). Dissected muscles were shock-frozen in liquid nitrogen and stored at −80°C until further analysis. Some muscles were also used directly after fresh dissection for intact fiber bundle mechanics (see below), whereas muscles to be used for single-fiber mechanics were stored at −20°C in 50% glycerol: 50% low ionic strength buffer (75 mM KCl, 10 mM Tris, 2 mM $MgCl_2$, 2 mM EGTA, 40 μg/ml protease inhibitor leupeptin, pH 7.1). Each muscle type was dissected at least twice (from two different animals).

### SDS-PAGE

Frozen skeletal muscles were homogenized in ice-cold salt buffer supplemented with 40 μg/ml leupeptin. For details, see Neagoe et al. (2002) and Opitz et al. (2004). After brief centrifugation, solubilization buffer (1% SDS, 1% 2-mercaptoethanol, 10% glycerol, 8 μg/ml leupeptin, 6 μM bromophenol blue, 4.3 mM Tris-HCl, pH 8.8, 4.3 mM EDTA) was added to the pellet, samples were incubated for 5 min on ice and boiled for 3 min.

Conventional 12.5% SDS-PAGE to separate proteins in the range of 15–220 kD was performed according to standard protocols. To investigate titin and nebulin isoforms, agarose-strengthened SDS-PAGE with a 2% polyacrylamide concentration was performed (Linke et al., 1997; Neagoe et al., 2002) using a Laemmli buffer system and a Biometra mini-gel system. To help estimate the molecular weight of titin isoforms, 2% SDS-PAGE lanes were loaded with a mix of muscle expressing titin of unknown size and the rabbit psoas muscle, which expresses two N2A-titin isoforms of ∼3.40 and 3.30 MD at a ratio of ∼30:70%. In sequencing studies, rabbit psoas titin has been predicted to be 3.40 MD (Freiburg et al., 2000). Using the psoas-titin bands as internal standards, the molecular mass of the titin band(s) of any muscle could be determined independent of size markers in adjacent gel lanes. Alternate lanes on a gel were loaded with psoas muscle alone, muscle with unknown titin size alone, or rat heart tissue, which provided another useful size marker at 3,000 kD (N2B-titin isoform), plus two faint cardiac N2BA-titin bands at 3,220 and 3,390 kD (Opitz et al., 2004; Warren et al., 2004). All gels were also loaded with rabbit soleus (titin, ∼3,600 kD) and some gels with human soleus (3,700 kD) and human heart tissue (N2B isoform, 3,000 kD; N2BA isoform, 3,300 kD) to obtain additional titin (and nebulin) size markers. We are grateful to Dr. R. Bittner (University of Vienna, Vienna, Austria) and Drs. Roger Hajjar and Federica del Monte (Massachusetts General Hospital, Boston, MA) for the gift of human soleus and human heart tissue, respectively. Attempts were made to load all lanes with equal amounts of solubilized protein after spectrophotometric analysis (Bradford method).

Protein bands were visualized with Coomassie brilliant blue or by silver staining, and gels were digitized by multiple scanning using a CanoScan 9900F scanner (Canon). Molecular weight calibration, measurements of titin size, and densitometry analyses were done using TotalLab software (Phoretix). A linear relationship between log $M_w$ and migration distance was assumed. Mean values (±SEM) of titin size were calculated from three to five observations per muscle type.

### Western Blotting

Immunoblotting to detect obscurin isoforms was done using chemiluminescent reaction kit (ECL system, Amersham Biosciences) according to standard protocols (Makarenko et al., 2004). Primary obscurin antibodies were α-I48/I49 and α-DH-domain, which were provided by M. Gautel (Young et al., 2001) and E. Ehler (King's College London, UK). Peroxidase-conjugated IgG served as secondary antibody.

### Single-fiber Mechanics

Single fibers 4–5 mm long were dissected from chemically skinned skeletal muscles previously stored in 50% glycerol: 50% low ionic strength buffer at −20°C for a maximum of 3 wk. We selected five muscles expressing different titin sizes, from small to large: psoas < EDL < gastrocnemius < longissimus dorsi < diaphragm. Except for the psoas, these muscles were found to express a single titin isoform. EDL and longissimus showed a similar proportion of slow fibers/MHC-I isoforms. Before dissection, muscles were skinned overnight in relaxing buffer (8 mM ATP, 10 mM phosphocreatine, 20 mM imidazole, 4 mM EGTA, 12 mM Mg-proprionate, 97 mM K-proprionate, 40 μg/ml leupeptin, pH 7.0, 180 mM ionic strength), to which 0.5% Triton X-100 had been added. Dissection was performed in relaxing buffer and care was taken to avoid excessive stretching of the fibers.

Mechanical measurements were made with a muscle mechanics workstation (Scientific Instruments; Minajeva et al., 2002; Opitz et al., 2003) at room temperature. Fibers were bathed in relaxing buffer (plus 40 μg/ml leupeptin, 30 mM 2,3-butanedione monoxime (BDM), an active force inhibitor, and 380 U/ml creatine kinase) and were attached to a motor arm and force transducer through stainless steel clips. Sarcomere length (SL) was measured by laser diffraction (Makarenko et al., 2004) using a 670-nm He-Ne laser. Only fibers with a clear diffraction pattern were used for mechanical measurements. Fibers were stretched from slack SL (2.0–2.2 μm) in six to seven steps of ∼0.2 μm/sarcomere (completed in 1 s) to a maximum SL, while SL was recorded during a 2-min pause after each step. Following the last stretch–hold, fibers were released back to slack SL to test for possible shifts of baseline force. Two identical stretch–release protocols were performed on one preparation; little differences were usually found between the recordings. From the recordings we measured the force at the end of each hold period and used these values to calculate force per cross-sectional area. The latter was estimated from the diameter of each sample (assuming a circular shape) measured in the nonstretched state under a binocular microscope using a 10-μm grid.

### Mechanical Measurements on Fiber Bundles

Fiber bundles 400–700 μm in diameter and 4–7 mm long were prepared from freshly excised muscles or deep-frozen tissue. Five muscles with increasing proportions of slow fibers/MHC-I were selected: psoas < EDL < gastrocnemius < diaphragm < soleus. Muscle strips were dissected as previously reported (Friden and Lieber, 2003) in a relaxing solution that prevents depolarization across any site of disrupted membrane and proteolytic degradation. In addition, the solution contained 20 mM BDM to fully relax the intact strips (Fryer et al., 1988) without affecting passive tension (Mutungi and Ranatunga, 1996); BDM also helps protect intact fibers from damage (Bagni et al., 2002). Alternatively some preparations were dissected and mechanically studied in standard Tyrode solution continuously bubbled with carbogen. Results of mechanical tests were similar for a given muscle in either type of solution.

Force and SL measurements (laser diffractometry) were performed in the apparatus also used for single-fiber studies. The stretch protocol was the same as described above. After measuring the stretch-dependent passive force of intact fiber bundles, the suspended muscle strip was skinned in relaxing buffer including 40 μg/ml leupeptin and 30 mM BDM, to which 0.5% wt/vol Triton X-100 had been added. During skinning, the experimental chamber was cooled down to ∼10°C and the skinning solution was stirred continuously using a magnetic bar. Skinning

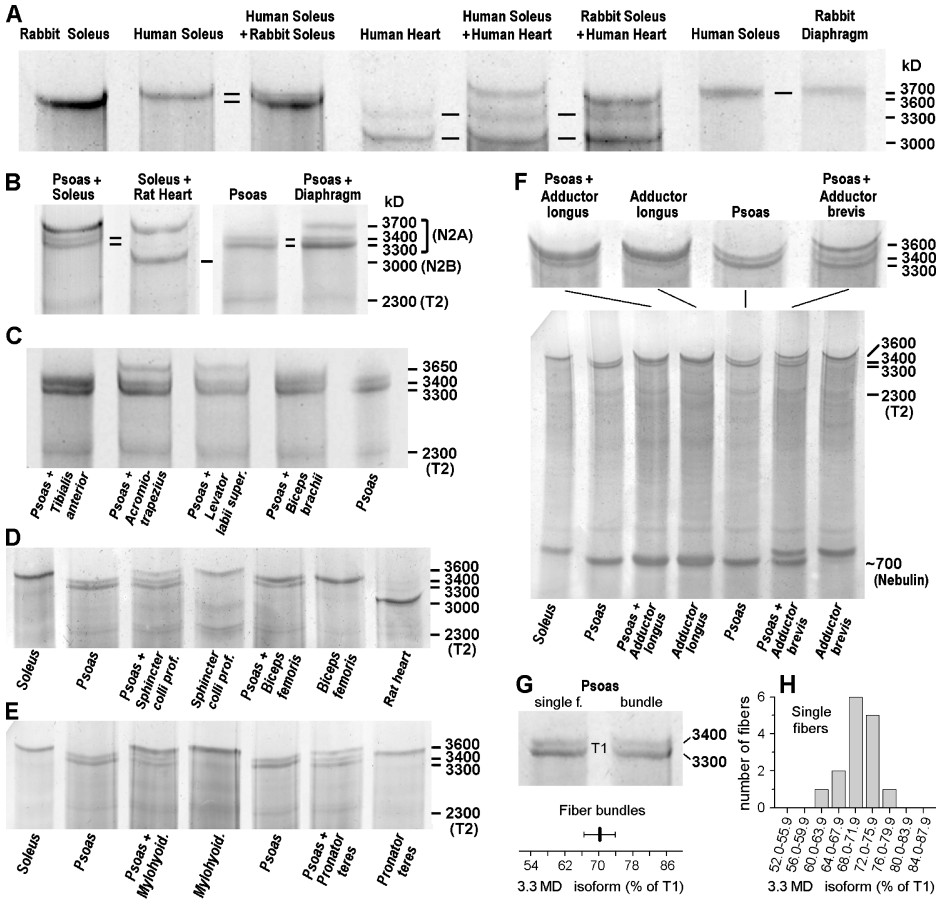


**Figure 2.** Detection of titin and nebulin isoforms by 2% SDS-PAGE. (A) Size comparison of rabbit muscle titins with sequenced human heart and soleus titins (Coomassie-stained gel). (B and C) Coomassie-stained gels showing up to two muscle samples charged to the same gel lane to obtain internal titin-size standards. Rabbit psoas expresses two isoforms of 3.4 and 3.3 MD at a ratio of 30:70; rat heart contains 3.0-MD titin. (D and E) Examples for titin appearance on silver-stained gels. (F) Silver-stained full gel also showing the nebulin bands and higher-magnification image of titin bands. (G) Comparison of titin isoform pattern in fiber bundles and in single fibers from rabbit psoas on Coomassie-stained gels. The proportion of 3.3-MD isoform was analyzed relative to the total T1-titin intensity (=combined 3.3 + 3.4-MD isoform intensity); the bottom panel shows mean ± SD for fiber bundles ($n$ = 10). (H) Histogram distribution of the 3.3-MD isoform percentage in 15 different single psoas fibers. T2, titin degradation band.

was completed after 4–6 h, when passive force development remained similar in two consecutive stretch protocols applied at a 30-min interval. Fiber bundles were then washed thoroughly with relaxing solution and passive force was recorded at room temperature. Finally, muscle strips were exposed to 0.2 μg trypsin/ml relaxing buffer (without leupeptin) for 45 min, which selectively proteolyzed titin, then the trypsin was washed out with relaxing buffer (plus leupeptin), and the same stretch protocol was repeated. For analysis, we again used the force at the end of each hold period (elastic force component).

To obtain force/cross-sectional area, the diameter of each sample was measured in the nonstretched state under a binocular microscope; a circular shape of the strip was assumed to calculate cross-sectional area. In addition, some bundles were fixed with 4% paraformaldehyde in relaxing buffer following the mechanical measurements and cross sections were cut with a microtome (Makarenko et al., 2004). The cross-sectional area, confirmed to be of near-circular shape, was determined in at least four sections cut along the fiber axis; the area varied by <12% among different sections of the same muscle strip. The measured areas compared reasonably well with the values calculated from the diameter of the specimens.

On quasi-steady-state passive tension versus SL plots, the data for each muscle were pooled in SL bins spaced 0.2 μm and mean passive tension values were calculated for all five muscle types, separately for intact, skinned, and titin-extracted preparations. Pooled data points for a given muscle were fitted by two-order polynomials. Passive stiffness was estimated from the area under the respective fit curves (integrals) as previously described (Makarenko et al., 2004). The unit of the stiffness thus calculated was N/m. The stiffness before skinning was taken as 100% (total stiffness).

## Single Myofibril Mechanics

Rabbit psoas and soleus myofibrils were isolated as previously described (Linke et al., 1996; Minajeva et al., 2001). In brief, thin muscle strips tied to glass rods were skinned in ice cold, low ionic strength buffer supplemented with 0.5% Triton X-100 for a minimum of 5 h. The skinned strips were minced and homogenized in rigor buffer to separate myofibrils.

A setup for myofibrillar force measurements has been previously described (Linke et al., 1997; Kulke et al., 2001). In brief, under a Carl Zeiss Axiovert 135 microscope, a myofibril was suspended between a glass needle attached to a piezomotor (Physik Instrumente) and another needle connected to a force transducer (homebuilt) with nanonewton resolution. Data collection and motor control were done with a PC, DAQ board, and custom-written LabView software (National Instruments). SLs were measured with a color-CCD camera (Sony), frame grabber, and Scion Image software (NIH) (Minajeva et al., 2002). Force measurements were performed at room temperature in relaxing buffer (Linke et al., 1994) supplemented with 30 mM BDM and 40 μg/ml leupeptin. The protocol consisted of stretching a nonactivated myofibril stepwise from slack SL by ~0.2 μm/sarcomere/step; each step was completed in 1 s. Following each step, the specimen was held at a constant SL for 20 s to wait for stress relaxation. For analysis we considered only the passive force at the end of the hold period, which represents titin-based force (Minajeva et al., 2001; Linke and Leake, 2004). To test for possible shifts of force baseline, myofibrils

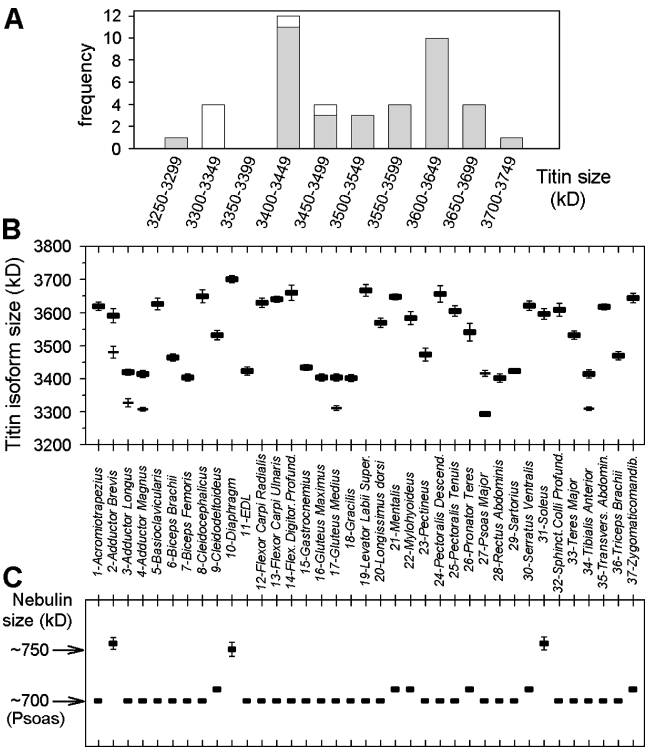


**Figure 3.** Titin and nebulin sizes in adult rabbit skeletal muscles. (A) Histogram of the titin-size distribution. Gray, major titin bands; white, minor titin bands. (B) Titin isoform size (mean ± SEM; $n$ = 3–5) in all 37 muscles studied. Thick bars, major titin; thin bars, minor titin. (C) Nebulin size (mean ± SEM) in comparison to the size of rabbit psoas nebulin estimated at ∼700 kD. Muscles are in alphabetical order.

were finally released back to slack SL. Force data were related to the cross-sectional area inferred from the diameter of the specimens (Linke et al., 1994).

### Modeling Titin-based Passive Force

Predictions for the shape of the force–extension curve of a given titin isoform were based on the assumption that overall single molecule titin elasticity could be modeled as two independent wormlike chains (WLCs) acting in series, corresponding to segments of tandem Ig domains and the PEVK region (Linke et al., 1998; Li et al., 2002). The WLC model of entropic elasticity (Marko and Siggia, 1995) predicts the relationship between the relative extension of a polymer ($z/L$) and the entropic restoring force ($f$) through

$$f = \left(\frac{k_B T}{A}\right)\left[\frac{1}{4(1 - z/L)^2} - \frac{1}{4} + \frac{z}{L}\right], \quad (1)$$

where $k_B$ is the Boltzmann constant, $T$ is absolute temperature (here, 300 K), $A$ is the persistence length (a measure of the bending rigidity of the chain), $z$ is the end-to-end length, and $L$ is the chain's contour length. For the titin segments, we used persistence length values of 10 nm (Ig domain regions) and 0.9 nm (PEVK domain), as suggested by Li et al. (2002). The contour lengths for the segments follow from the number of domains/residues in each segment and the maximum length of one domain (4.5 nm) or residue (0.36 nm). Unfolding of proximal Ig domains was modeled as a two-state process (folded and unfolded) according to Rief et al. (1997) and Kellermayer et al. (1997). Unfolding of distal Ig domains was excluded within the force range modeled.

The force developed by a single titin molecule upon extension of a myofibril was predicted using the following size values for skeletal titin isoforms: (a) 3,700 kD, the size of human-soleus titin containing 90 (68 proximal, 22 distal) Ig domains and 2,200 PEVK residues in the molecule's elastic I band part (Labeit and Kolmerer, 1995), and (b) a mix of 3,400 kD (30% weight) and 3,300 kD (70% weight) isoforms, which mimicks the situation in rabbit psoas. Psoas titin was assumed to contain 72 (50 proximal, 22 distal) Ig domains and 800 PEVK residues in the 3,400-kD isoform (Freiburg et al., 2000) and 65 (43 proximal, 22 distal) Ig domains and 650 PEVK residues in the 3,300-kD isoform. For other parameters in the simulation, see Li et al. (2002).

### Electron Microscopy

Intact and triton-skinned plus trypsin-treated rabbit psoas and soleus muscle strips (following mechanical measurements) were fixed in 4% paraformaldehyde (in relaxing buffer), dehydrated in an alcohol series, and embedded in Epon blocks. Cross sections or longitudinal sections were cut using a Reichert ultramicrotome. Contrasted sections were then used for transmission electron microscopy performed with a Carl Zeiss EM 900 at 80 kV. Of main interest were the collagen depositions in between the muscle fibers.

### Histology and Myosin ATPase Staining

Small strips of muscle tissue were incubated in 4% paraformaldehyde overnight. Then the strips were attached to the plates of a cryosectioning device (MICROM HM-500-O) using frozen section medium (Neg–50; Richard-Allan Scientific). 20-μm-thick serial transverse sections were cut at −18°C, recovered on a gelatin-coated glass slide, and dried. Myosin ATPase staining was performed following a protocol by Hamalainen and Pette (1993). Preincubation time was 15 min at pH 4.5 (room temperature) and incubation time was 45 min at pH 9.4 (37°C). In these acid-ATPase–stained sections, dark fibers were classified as type-I and lighter fibers as type-II. Type-IIA fibers appeared white, whereas type-IIB or IID fibers were stained gray (Lind and Kernell, 1991). Following staining, sections on slides were sealed with EUKITT and topped with a coverslip. For some sections we also used alkaline preincubation at pH 9.4 and generally confirmed the fiber type classification obtained by acid preincubation (not depicted).

Analysis of fiber types was done under a Leitz Orthomat-W microscope and pictures were taken with a camera on Elite chrome Kodak film. For microscopic analysis, we selected an area comprising 50 fibers on a given section and determined the percentage of fiber types. Two different areas on each section and two different serial sections were analyzed for each skeletal muscle and the averages and error estimates of the four areas were calculated.

### MHC Typing by Gel Electrophoresis

MHC isoforms were separated on 8% SDS-PAGE containing 30% glycerol according to the method of Talmadge and Roy (1993). A Biometra minigel system was used for electrophoresis and was kept on ice during separation. A constant voltage of 70 V was applied over a 30-h running time. Gels were stained with Coomassie brilliant blue.

Each rabbit muscle type was analyzed a minimum of four times and the average composition of myosin types was calculated. The percentage of MHC types I, IIB, IID, and IIA was determined by densitometric analysis using TotalLab software (Phoretix). Although the gels allowed separation of the bands for MHC-IID and MHC-IIA, we chose to combine these two MHC types in the analysis, as their contractile properties are more similar to one another than to those of the other MHC isoforms (Andruchov et al., 2004).

TABLE I

*Fiber Type and MHC Isoform Composition, as well as Titin Size(s), in 37 Rabbit Skeletal Muscles*

| Muscle name | %I fibers | %IIA fibers | %IIB/D fibers | %I MHC | %IIA/D MHC | %IIB MHC | Titin size (kD) major band (mean ± SEM) | Titin size (kD) minor band (mean ± SEM) | References |
|---|---|---|---|---|---|---|---|---|---|
| Acromiotrapezius | 6.1 | 93.9 | 0 | 11.3 | 88.7 | 0 | 3,620 ± 12 | – | |
| Adductor brevis | 97.5 | 0 | 1.5 | 98.4 | 1 | 0.6 | 3,590 ± 21 | 3,480 ± 17 | Hitomi et al., 2005 |
| Adductor longus | 7.7 | 90.3 | 2 | 0 | 38 | 62 | 3,420 ± 6 | 3,328 ± 11 | Joosten et al., 1981 |
| Adductor magnus | 0 | 2.4 | 97.6 | 0 | 25.3 | 74.7 | 3,413 ± 9 | 3,307 ± 3 | Joosten et al., 1981; Aigner et al., 1993; Hamalainen and Pette, 1993; Rab et al., 2000 |
| Basioclavicularis | 17.5 | 82.5 | 0 | 14.7 | 85.3 | 0 | 3,627 ± 18 | – | |
| Biceps brachii | 12.2 | 0 | 87.8 | 6.3 | 84.2 | 9.5 | 3,465 ± 10 | – | Fuentes et al., 1998 |
| Biceps femoris | 0 | 87.5 | 12.5 | 0 | 58.5 | 41.5 | 3,405 ± 9 | – | Gondret et al., 1996 |
| Cleidocephalicus | 10.5 | 88.5 | 1 | 1 | 99 | 0 | 3,648 ± 19 | – | |
| Cleidodeltoideus | 22.5 | 77.5 | 0 | 4.7 | 95.3 | 0 | 3,530 ± 15 | – | |
| Diaphragm | 51 | 37 | 12 | 53.4 | 46.6 | 0 | 3,700 ± 9 | – | Aigner et al., 1993; Jimenez-Fuentes et al., 1998; Le Souef et al., 1988; Capdevila et al., 2003 |
| EDL | 4.4 | 31.6 | 64 | 3 | 97 | 0 | 3,425 ± 10 | – | Lobley et al., 1977; Aigner et al., 1993; Hamalainen and Pette, 1993; Lexell et al., 1994; Wang and Kernell, 2001 |
| Flexor carpi radialis | 22.5 | 70 | 7.5 | 14.7 | 85.3 | 0 | 3,630 ± 15 | – | |
| Flexor carpi ulnaris | 15.1 | 84.9 | 0 | 15.5 | 84.5 | 0 | 3,640 ± 6 | – | |
| Flexor digitorum profundus | 14.1 | 85.9 | 0 | 12.3 | 87.7 | 0 | 3,660 ± 23 | – | |
| Gastrocnemius | 14.8 | 15.2 | 70 | 14.3 | 85.7 | 0 | 3,435 ± 6 | – | Aigner et al., 1993; Hamalainen and Pette, 1993; Wang and Kernell, 2001; Pagliassotti and Donovan, 1990 |
| Gluteus maximus | 4.5 | 88.5 | 7 | 0 | 6.7 | 93.3 | 3,405 ± 6 | – | |
| Gluteus medius | 3.5 | 92.7 | 3.8 | 0 | 25.3 | 74.7 | 3,405 ± 6 | 3,310 ± 6 | Joosten et al., 1981 |
| Gracilis | ND | ND | ND | 0 | 99.5 | 0.5 | 3,403 ± 9 | – | Rouanet and Bacou, 1993; Joosten et al., 1981; Pagliassotti and Donovan, 1990 |
| Levator labii superior | 16 | 0 | 84 | 8 | 92 | 0 | 3,667 ± 18 | – | |
| Longissimus dorsi | 5.1 | 4.9 | 90 | 5.5 | 94.5 | 0 | 3,570 ± 15 | – | Vigneron et al., 1976; Lobley et al., 1977; Gondret et al., 1996; Lutz et al., 1978 |
| Mentalis | 24.5 | 75.5 | 0 | 14.3 | 85.7 | 0 | 3,650 ± 6 | – | |
| Mylohyoideus | 31.7 | 34.3 | 34 | 19 | 81 | 0 | 3,583 ± 19 | – | |
| Pectineus | 8.9 | 91.1 | 0 | 9.4 | 90.6 | 0 | 3,473 ± 20 | – | |
| Pectoralis descendens | 33.6 | 29.1 | 37.3 | 24 | 76 | 0 | 3,655 ± 26 | – | Frey et al., 1998 |
| Pectoralis tenuis | 22.1 | 87.9 | 0 | 39.5 | 60.5 | 0 | 3,605 ± 16 | – | |
| Pronator teres | 11.5 | 77.5 | 11.5 | 7 | 93 | 0 | 3,540 ± 26 | – | |

TABLE I

*Fiber Type and MHC Isoform Composition, as well as Titin Size(s), in 37 Rabbit Skeletal Muscles (Continued)*

| Muscle name | %I fibers | %IIA fibers | %IIB/D fibers | %I MHC | %IIA/D MHC | %IIB MHC | Titin size (kD) major band (mean ± SEM) | Titin size (kD) minor band (mean ± SEM) | References |
|---|---|---|---|---|---|---|---|---|---|
| Psoas major | 0 | 0 | 100 | 0 | 100 | 0 | 3,295 ± 6 | 3,416 ± 8 | Lobley et al., 1977; Aigner et al., 1993; Hamalainen and Pette, 1993; Gondret et al., 1996; Tikunov et al., 2001 |
| Rectus abdominis | 19.5 | 64.5 | 16 | 20 | 80 | 0 | 3,400 ± 12 | – | |
| Sartorius | 5 | 90 | 5 | 1.6 | 77.4 | 21 | 3,425 ± 3 | – | Joosten et al., 1981 |
| Serratus ventralis | 11.5 | 88.5 | 0 | 25 | 75 | 0 | 3,622 ± 13 | – | |
| Soleus | 91.8 | 0 | 8.2 | 94.5 | 5.5 | 0 | 3,596 ± 17 | – | Lobley et al., 1977; Lutz et al., 1978; Pagliassotti and Donovan, 1990; Aigner et al., 1993; Lexell et al., 1994; Wang and Kernell, 2001; Tikunov et al., 2001 |
| Sphincter colli profundus | ND | ND | ND | 0 | 100 | 0 | 3,608 ± 19 | – | |
| Teres major | 21.9 | 78.1 | 0 | 17.7 | 82.3 | 0 | 3,530 ± 12 | – | |
| Tibialis anterior | 4.5 | 92.5 | 3 | 2.3 | 97.7 | 0 | 3,414 ± 12 | 3,308 ± 4 | Lobley et al., 1977; Aigner et al., 1993; Hamalainen and Pette, 1993; Mabuchi et al., 1982; Wang and Kernell, 2001; Yamazaki et al., 2003 |
| Transversus abdominis | 24.7 | 70.3 | 5 | 26.5 | 73.5 | 0 | 3,617 ± 9 | – | |
| Triceps brachii | 7.7 | 92.3 | 0 | 2 | 88 | 10 | 3,470 ± 12 | – | Fuentes et al., 1998 |
| Zygomatico-mandibularis | 26.8 | 73.2 | 0 | 15.7 | 84.3 | 0 | 3,643 ± 15 | – | |

Titin size is an average of three to five observations per muscle. A reference list for fiber/MHC composition in rabbit muscles is included (right column).

### Regression Analysis

Linear regression analysis was performed to detect correlations between mean titin size and fiber/MHC composition. Similarly, obscurin size was related to titin size and the type-I fiber/MHC-I proportions. Estimates for a statistically significant relationship were based on standard criteria: correlation coefficient, $R \leq 0.3$, no correlation; $0.3 < R < 0.7$, low to modest correlation; $R \geq 0.7$, high correlation. The P value in the regression analysis had to be below 0.05 for the correlation to be judged significant.

## RESULTS

### Titin Size Varies Greatly in Rabbit Skeletal Muscles

The size of rabbit titin isoforms was determined by 2% SDS-PAGE by comparison with the molecular masses of sequenced human titins (Fig. 2 A). Rabbit soleus was found to be ~100 kD smaller than human soleus, which was also apparent by comparison with human heart titin expressing 3.0-MD N2B isoform and ~3.3-MD N2BA isoforms (Fig. 2 A). Intact (T1) N2A-titin showed a broad size distribution in the set of 37 rabbit skeletal muscles, ranging from ~3.3 to 3.7 MD (Fig. 2, A–F). No single prevailing titin size was apparent on a histogram plot of the binned size distribution, although the majority of muscles had titin sizes between either 3.40–3.45 MD or 3.60–3.65 MD (Fig. 3 A). 31 muscles exhibited a single titin isoform (Fig. 2; Fig. 3, A and B), including the gastrocnemius, which has obvious red and white portions. Another muscle that contains two portions differing greatly in type-I fiber content, the tibialis anterior (Mabuchi et al., 1982), showed two isoforms separated by ~100 kD (Fig. 3 B). Two titin isoforms were detected in 6 of the 37 muscles,

also in the psoas, the three hindlimb adductor muscles (longus, brevis, and magnus), and the gluteus medius (Fig. 2 F; Fig. 3 B). In all but one (the psoas) muscle expressing two titin bands, the lower-mobility protein appeared much stronger than the higher-mobility protein. The T2-titin bands, which are considered to be degradation forms of the intact titin molecule, were generally weak on the gels and only rarely made up >15% of the intensity of the T1-titin bands (Fig. 2).

The titin size values of individual muscles are listed in Table I. The shortest major isoform was detected in psoas (~3,300 kD), the largest isoform in diaphragm (3,700 kD), similar to human soleus titin (Fig. 2 A). Also many facial muscles (levator labii superior, mentalis, sphincter colli profundus, zygomaticomandibularis; range of mean sizes, 3,608–3,667 kD) predominantly express long titins. Otherwise we did not find any obvious clustering of long or short titins depending on body location.

Often muscles are arranged such that contraction of one muscle, the agonist, stretches its counterpart, the antagonist, the extension of which is determined by the passive mechanical properties. We therefore searched for preferential patterns of titin expression in agonist–antagonist pairs. However, no such patterns were apparent: (a) the biceps brachii (agonist) and the triceps brachii (antagonist) express the same titin size (3,465 ± 10 versus 3,470 ± 12 kD); (b) agonists with a similar size of the major titin isoform, the tibialis anterior (3,414 ± 12 kD) and EDL (3,425 ± 10 kD), oppose antagonists that differ in titin size, the soleus (3,596 ± 17 kD) and gastrocnemius (3,435 ± 6 kD); (c) the muscle group that includes the hindlimb adductors (a. longus, 3,420 ± 6 kD; a. magnus, 3,413 ± 9 kD), the pectineus (3,473 ± 20 kD), and the gracilis (3,403 ± 9 kD), which all express a rather short major titin isoform, is antagonist to the glutei, which both contain also a short 3,405-kD titin; and (d) the teres major has titin of 3,530 ± 12 kD, whereas the muscles of the antagonist group can express a similar size titin ([cleido]deltoideus, 3,530 ± 15 kD) or larger titins (pectoralis, mean size, 3,605–3,655 kD; [acromio]trapezius, 3,620 ± 12 kD). There is no predictable pattern of titin size expression in agonist–antagonist muscle systems.

### Individual Fibers in a Muscle Show a Similar Titin Isoform Expression Pattern

Since the vast majority of rabbit muscles express a single titin isoform, the same isoform must be present in all individual fibers of a given muscle. Analysis of titin size at the single-fiber level was therefore deemed unnecessary in these muscles. However, we wanted to know the isoform composition in a muscle expressing two titin sizes, such as the psoas, at the single-fiber level.

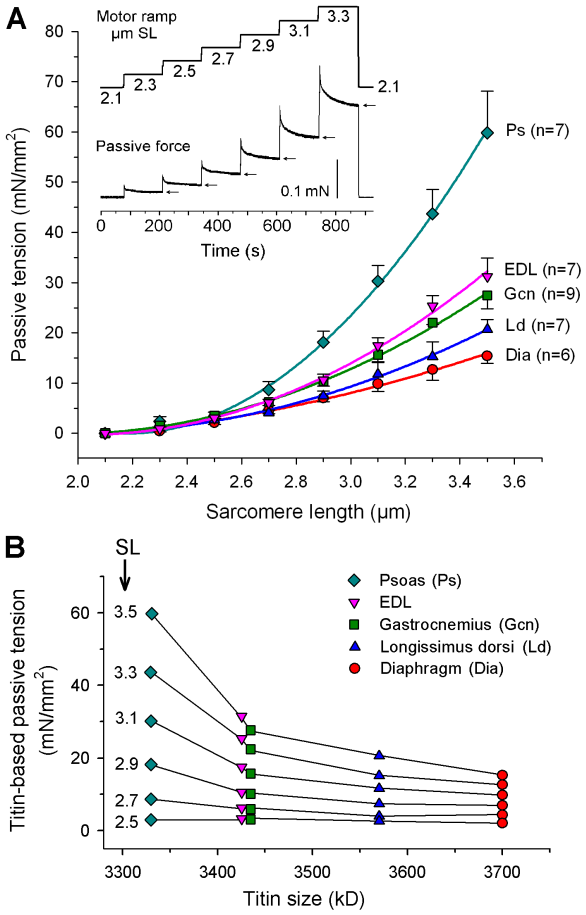


**Figure 4.** Passive tension of single muscle fibers correlates inversely with titin size. (A) Passive SL–tension curves of single fibers from five different triton-skinned rabbit muscles. Data are means ± SEM. Curves are second-order polynomial fits. Inset, mechanics protocol. Arrows indicate quasi-steady-state force, which was used to calculate PT in the main figure. (B) Single-fiber (titin-based) mean PT at a given sarcomere length (µm; indicated left to each curve) plotted against titin size of the respective rabbit muscles.

15 different single psoas fibers were studied by 2% SDS-PAGE and all of them revealed a doublet titin band (Fig. 2, G and H). The proportion of the major 3.3-MD isoform varied somewhat in these fibers (range, 61–79%; Fig. 2 H), but the mean proportion of 70.5 ± 4.4% (mean ± SD) was identical to that measured in chunks of psoas muscle tissue (Fig. 2 G), 70.4 ± 3.8% ($n$ = 10). Thus, individual psoas fibers all contain two titin isoforms and express these isoforms at a similar ratio.

### Nebulin Size Shows Low Variability but Is Increased in Predominantly Slow Muscles

An abundant giant protein in skeletal muscle is nebulin, a thin filament length ruler (Kruger et al., 1991; Labeit et al., 1991; Pfuhl et al., 1994; McElhinny et al., 2005). Analysis of nebulin-size expression in the 37 rabbit muscles revealed much less variability than for titin

(Fig. 3 C). Only three muscles (soleus, diaphragm, and adductor brevis) showed a significantly increased (by 50–70 kD) nebulin size compared with the psoas nebulin band, which served as a reference band estimated at ~700 kD (Fig. 2 F). Those three muscles were the only muscles containing >50% type-I MHC or >50% type-I fibers (Table I).

### Titin Size Differences Translate into Large Differences in Titin-based Passive Tension

To determine how the variability in titin size expression affects titin-based PT, we measured the passive SL–tension curves of single skinned fibers of psoas, EDL, gastrocnemius, longissimus dorsi, and diaphragm muscles (Fig. 4 A). The lowest PT was seen in the slow diaphragm expressing 3,700-kD titin isoform. Among the other muscles (which are predominantly fast in rabbit; Table I), distinct differences in PT levels were found: longissimus exhibited the lowest PT, EDL and gastrocnemius intermediate PT, and psoas the highest PT (Fig. 4 A). These differences become obvious >~2.7–2.9 μm SL and reflect the expression of different-size titins in those muscles (Fig. 4 B). Muscles with a similar proportion of MHC-I isoforms, such as EDL and longissimus (Table I), differed markedly in PT. The data shows (a) that the passive stiffness of fibers scales inversely with titin size and (b) that fast muscle fibers can have either high or low PT levels.

To confirm that differences in fiber PT arise from differences in myofibrillar PT, passive SL–tension relationships were obtained from single isolated myofibrils of rabbit psoas and soleus muscle (Fig. 5). The mean PT was larger in psoas than in soleus myofibrils by a factor of ~1.2 (not statistically significant in Student's $t$ test), 3.0, and 3.4 (both statistically significant at $P < 0.05$), at 2.3, 2.7, and 3.1 μm SL, respectively (Fig. 5 B, symbols). These differences are comparable to those reported for rabbit soleus and psoas at the single-fiber level (Horowits, 1992).

We wanted to know whether the measured PT difference is in a range that can, in theory, be expected from the observed variations in titin size. Therefore we modeled the force per titin molecule using an approach described earlier (Li et al., 2002; Makarenko et al., 2004), which is based on the wormlike chain properties of the titin spring. Different domain compositions in titin's elastic I-band segment were assumed based on sequence information (see MATERIALS AND METHODS), corresponding to short titin isoforms (as in psoas) or long titin (as in soleus). The force differences were predicted to be low at small extensions but increase at higher extensions and were qualitatively similar to the measured differences at the myofibril level (Fig. 5 B, curves). The modeled force curves essentially represent the boundaries for the titin-based force differences that can be expected from the titin size variability.

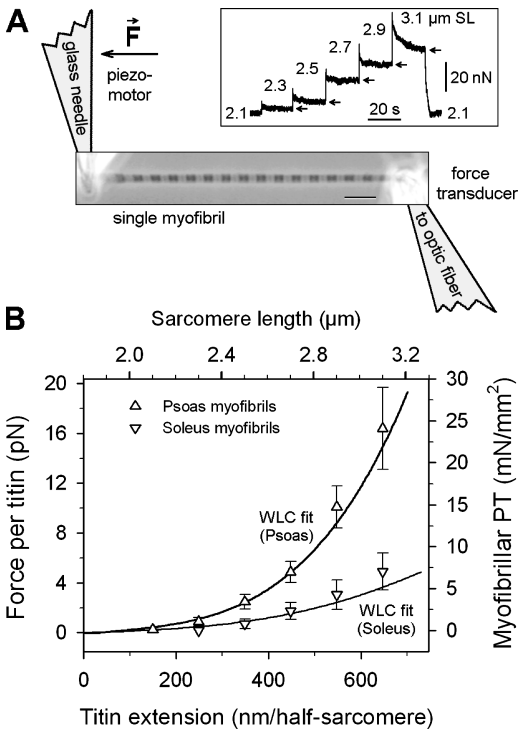


**Figure 5.** Range of variability in titin-based passive force due to titin-size differences estimated by single-myofibril mechanics and wormlike chain simulations. (A) Scheme of experimental arrangement for mechanical manipulation of single myofibrils. Bar, 5 μm. Inset, typical force trace during stepwise stretch of myofibril. Arrows indicate quasi-steady-state (elastic) force. (B) Differences in titin-based force between myofibrils expressing longer titin (soleus) and those expressing short titins (psoas). Symbols (mean ± SEM) correspond to the right and top axes and indicate the elastic component of PT in single myofibrils. Lines correspond to the left and bottom axes and show wormlike chain predictions of force per titin molecule, for a muscle expressing short titins (30:70 mix of 3.4/3.3 MD isoforms, as in rabbit psoas) in comparison to a muscle expressing long titin (3.7 MD; as in human soleus or rabbit diaphragm). Titin extensions of 0–700 nm mimick the SL range 1.8–3.2 μm. The curves show the maximum and minimum forces that are to be expected from the titin size variability in rabbit muscles.

### Fiber Types and Myosin Heavy Chain Isoforms in Rabbit Skeletal Muscles

In the set of rabbit skeletal muscles we also determined the fiber type and MHC isoform compositions. Myofibrillar ATPase staining of transverse serial cryosections after preincubation at pH 4.5 (Fig. 6 A) distinguished type-I fibers (black staining) from type-II fibers (lighter staining), which again could be subclassified in type-IIA (white appearance) and type-IID or IIB fibers (greyish staining). The MHC types were determined by 8% SDS-PAGE, which resolved the isoforms I, IIB, IID, and IIA (Fig. 6 B). The mean percentages of fiber types

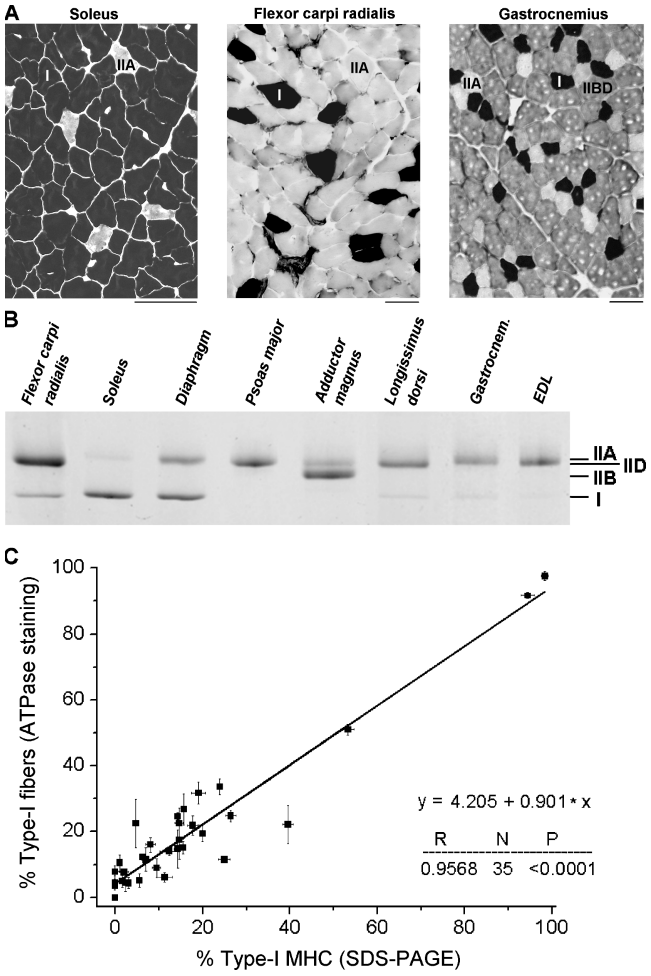


**Figure 6.** Fiber and myosin typing. (A) Detection of fiber types I, IIA, and IIB or IID by myosin ATPase staining of 20-μm-thick transverse cryosections preincubated at pH 4.5. Bars, 100 μm. (B) Myosin heavy chain isoforms I, IIB, IID/IIA discriminated by 8% SDS-PAGE. (C) Correlation between type-I fiber composition and MHC-I isoform percentage of 35 rabbit skeletal muscles (for two muscles ATPase staining was not determined). Data are mean ± SEM. The line is a linear regression; results are shown in the lower right corner.

and MHC isoforms in each muscle are listed in Table I. There was a good correlation (coefficient, R = 0.957) between type-I fiber percentage and type-I MHC percentage (Fig. 6 C). Most rabbit muscles contained a majority of type-II fibers or type-II MHCs and thus were classified as predominantly fast (34 muscles). Only three muscles were predominantly slow, containing >50% type-I fiber/MHC types: soleus, diaphragm, and adductor brevis. The fiber-type or MHC-type proportions measured by us were usually consistent with those reported by others for a given rabbit muscle. (An exception was the gracilis muscle, which contained 99.5% type IIA/IID MHC and not, as reported by Pagliassotti and Donovan (1990), almost exclusively type-IIB MHC.) A list of references on MHC/fiber type composition in rabbit muscles has been added to Table I (right column).

### Fast Muscles Express either Short or Long Titin(s), Slow Muscles Only Long Titin

On plots of titin size (major band only) versus percentage of fiber type or MHC isoform (Fig. 7), we found a modest, statistically significant correlation with the type-I fibers and type-I MHCs (Fig. 7, A and D). As for type-I fibers (Fig. 7 A), the correlation coefficient, R, was 0.447 ($P = 0.007$; $n = 35$) if all muscles were included in the analysis and 0.651 ($P < 0.0001$; $n = 32$) if the three slow muscles were excluded. When titin size was plotted against percentage of MHC-I (Fig. 7 D), R was 0.412 ($P = 0.011$; $n = 37$; all muscles included) and 0.554 ($P = 0.0007$; $n = 34$; slow muscles excluded), respectively. In contrast, no relationships were found between titin size and the relative content of type-IIA fibers (Fig. 7 B), type-IIB/IID fibers (Fig. 7 C), or type-IIA/IID MHC (Fig. 7 E). There were only 10 muscles that actually contained type-IIB MHC, confirming earlier observations that only a minority of rabbit muscles contains type-IIB MHC (Aigner et al., 1993), and titin size did not correlate with the percentage of MHC-IIB in these muscles (Fig. 7 F).

In these experiments we chose not to study single fibers but muscle chunks, because the aim was a correlation with the titin isoforms and because we had found that most muscles (31 out of 37) contain only a single titin isoform. In these muscles, a single titin isoform must be present in all individual fibers. Since many of these muscles contain different fiber/MHC types, we also know that the different fiber types in a given muscle nevertheless contain the same titin isoform. The one muscle studied for titin isoforms at the single-fiber level, the psoas, contained 100% type-IID fibers/MHC, in agreement with Hamalainen and Pette (1993). Since individual psoas fibers express 3.4-MD and 3.3-MD titin isoforms at a similar ratio (Fig. 2, G and H), the MHC/fiber type versus titin isoform relationship is established unambiguously. In the remaining five muscles showing a titin doublet on gels, the minor titin band was always very faint (e.g., Fig. 2 F, Adductor longus) and it was considered sufficient to correlate the fiber/MHC type only with the major titin isoform (Fig. 7).

Taken together the data suggest that fiber type or MHC isoform are weak indicators of titin size. Clearly, fast muscles can express either short or long titin isoforms. However, Fig. 7 (A and D) also shows that muscles with a type-I fiber content ≥23% or those with a MHC-I content >20%, i.e., the predominantly slow muscles and the slower ones among the fast muscles, all contain relatively large titin isoform(s) >3,580 kD.

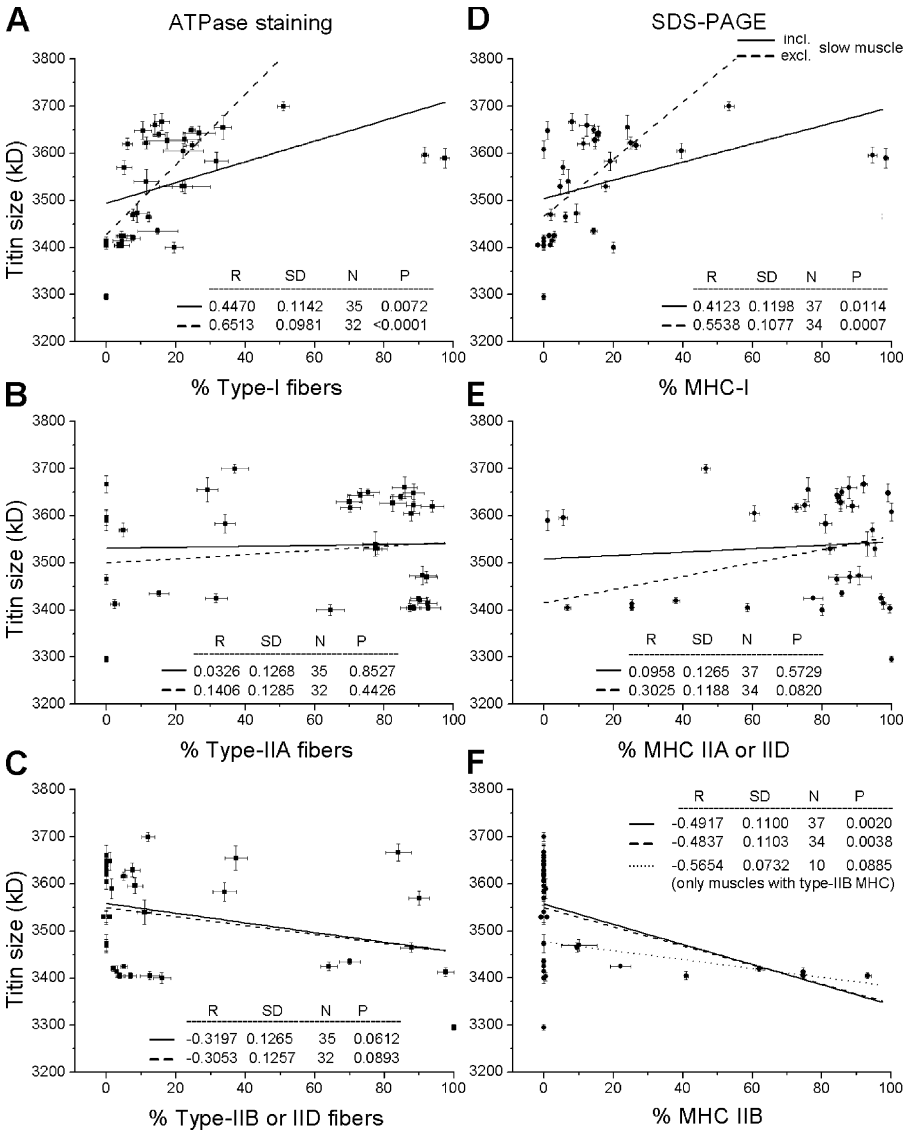


**Figure 7.** Relationships between titin size and muscle fiber type or MHC isoform percentage determined by myofibrillar ATPase staining (left) and 8% SDS-PAGE (right). Lines are linear regressions (results are shown in each panel). Correlations were made with (A) type-I, (B) type-IIA, (C) type-IIB or IID fibers, and (D) type-I, (E) type-IIA or IID, (F) type-IIB MHC. Dashed lines are regressions after omitting data points for muscles containing >50% type-I fibers or type-I MHC (=slow muscles). The dotted line in F is a regression to the data points of the 10 muscles with MHC-IIB content above zero. Only the major titin band was included in the analysis. Data are means ± SEM.

### Titin-based Stiffness Contributes Significantly to Total Passive Muscle Stiffness

Mechanical measurements were performed on fiber bundles dissected from five rabbit muscles differing greatly in fiber-type/MHC composition (psoas, soleus, gastrocnemius, EDL, and diaphragm) to determine to what degree titin contributes to total passive muscle stiffness. The quasi-steady-state PT was first recorded in intact fiber bundles, then in chemically skinned fibers, and finally after proteolytic digestion of titin (Fig. 8). As a measure of passive stiffness, we calculated the integrals under the fit curves to the pooled data points (intact fiber stiffness = 100%).

After skinning, the passive stiffness was reduced in all muscle types (dashed curves in Fig. 8, A–E); the highest relative stiffness decrease (by 37%) occurred in soleus, the smallest decrease (by ~24%) in gastrocnemius. The stiffness decrease upon triton treatment was unlikely to be due to titin modifications, because we found the titin expression patterns on 2% SDS-PAGE gels to be unchanged in skinned compared with intact muscles (examples in Fig. 9 A), Rather, it may be the mechanical uncoupling between muscle fibers and the connective tissue and some removal of extracellular material during skinning that account for the decreased passive stiffness.

We then tested the effect of selective degradation of titin by low doses of trypsin on PT (Fig. 8, A–E). Minute concentrations of trypsin disrupt titin but have no measurable effect on other muscle proteins (Funatsu et al., 1990; Higuchi, 1992; Helmes et al., 2003). The trypsin effect was confirmed here: titin was readily proteolyzed by 0.2 μg/ml trypsin applied for 45 min (Fig. 9 A), but other muscle proteins remained unchanged as judged by 12.5% SDS-PAGE (Fig. 9 B). Following titin proteolysis, the PT of the five muscles dropped by different

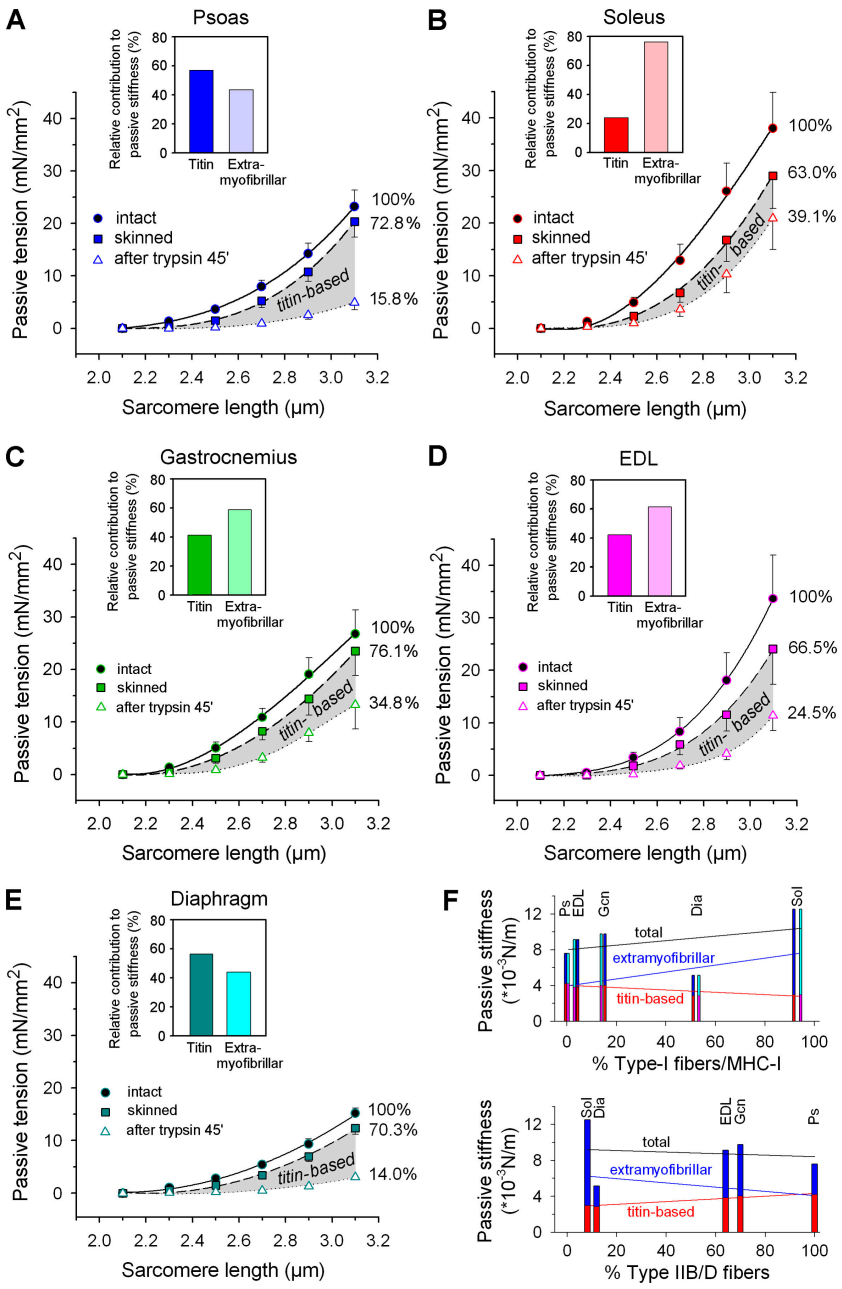


**Figure 8.** Contribution of titin to total passive stiffness in different muscle types. (A–E) Passive SL–tension curves of muscle strips before (circles; solid curve) and after (squares; dashed curve) skinning with Triton X-100, and following 45-min-long treatment with 0.2 µg/ml trypsin to disrupt titin (triangles; dotted curve). Data points are means ± SEM. Numbers next to curves indicate the remaining relative stiffness after the respective chemical treatments; passive stiffness was calculated from the integrals below the two-order polynomial fit curves. Insets, relative contributions from titin and extramyofibrillar elements to total passive muscle stiffness. (A) Psoas ($n$ = 10), (B) soleus ($n$ = 11), (C) gastrocnemius ($n$ = 5), (D) EDL ($n$ = 5), (E) diaphragm muscle ($n$ = 5). (F) Relationships of total, titin-based, and extramyofibrillar passive stiffness with the relative type-I fiber/MHC-I content (top; MHC, cyan and pink; fibers, blue and red color) and the relative type-IIB/D fiber content (bottom) of the five muscles. Fit curves are linear regressions. Statistically significant correlations were found only for titin-based stiffness: type-I fibers, R = −0.8801, P = 0.0489; MHC-I, R = −0.8834, P = 0.0469; type-IIB/D fibers, R = 0.9806, P = 0.0032.

amounts (reflecting the differences in titin-based stiffness), but still remained much above zero. In psoas and diaphragm, only 15.8% and 14.0%, respectively, of the total (intact muscle) stiffness remained, much less than in soleus (39.1%) and gastrocnemius (34.8%) (dotted curves in Fig. 8, A–C and E). A source of this residual stiffness is unlikely to be intermediate filaments, as they contribute to PT only at SLs >3.4 µm (Salviati et al., 1990; Wang et al., 1993). Rather, collagen fibers surrounding the muscle cells are suggested to be the main cause of the residual stiffness. Indeed, on electron micrographs of psoas and soleus fiber bundles we detected abundant collagen depositions in both intact and skinned/trypsin-treated muscle strips (Fig. 10). However, the collagen network was much more extensive in soleus than in psoas, at both experimental stages (Fig. 10). The higher abundance of collagen fibers in soleus may explain the greater residual stiffness in this muscle compared with psoas.

These results show that titin's relative contribution to total passive stiffness is much higher in some muscles, like psoas (57%) and diaphragm (~56%), than in others, like soleus (~24%), EDL (42%), and gastrocnemius (~41%). Another significant stiffness component comes from the extramyofibrillar structures, including collagen (Fig. 8, A–E, insets). Hence, both extrasarco-

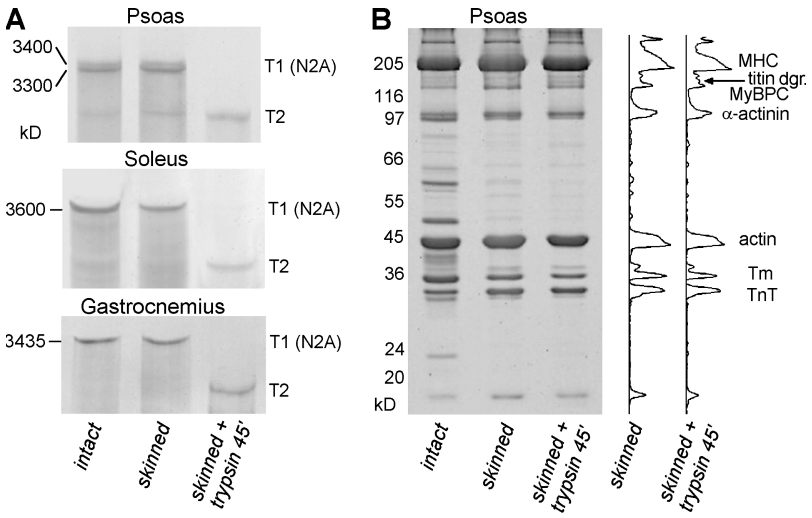


**Figure 9.** Effect of skinning and low trypsin (0.2 μg/ml) treatment on rabbit muscle proteins. (A) 2% SDS-PAGE for titin in psoas, soleus, and gastrocnemius. T1, intact titin; T2, titin degradation band. (B) 12.5% SDS-PAGE and intensity profiles showing no change of protein bands other than titin after low-trypsin treatment of skinned psoas muscle.

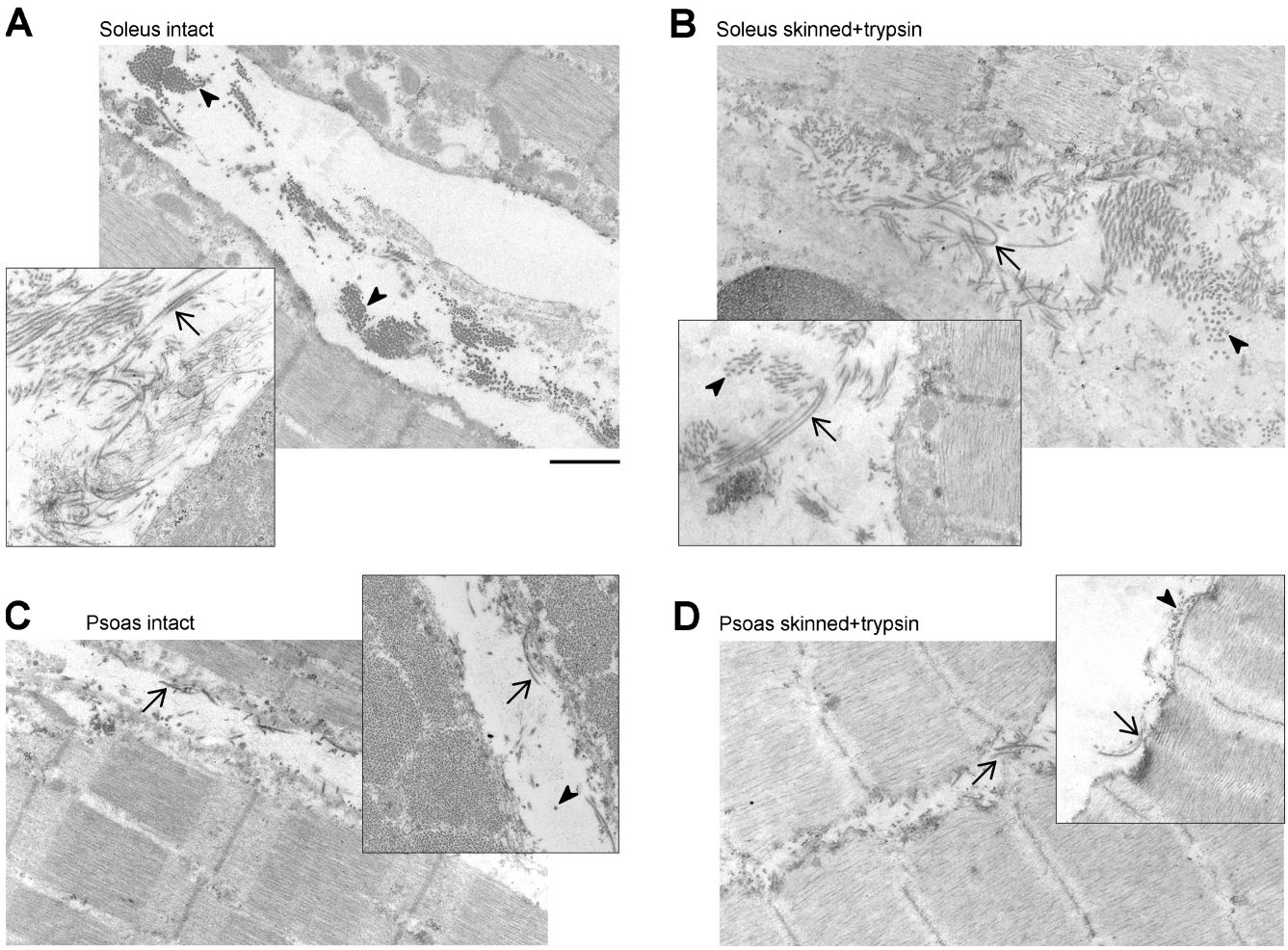


**Figure 10.** Collagen fibers in rabbit psoas and soleus. Representative electron micrographs of muscle strips before (A and C) and after (B and D) exposure to Triton X-100 (skinning) and 0.2 μg/ml trypsin (titin proteolysis), in soleus (A and B) and psoas (C and D). Note the extensive collagen depositions in intact soleus, which are barely removed during skinning. Psoas contains much less collagen than soleus. Mechanical measurements had been performed on the treated fiber bundles before preparation for EM. Arrowheads, collagen fibers in cross section; arrows, in longitudinal section. Bar, 1 μm (for all panels).

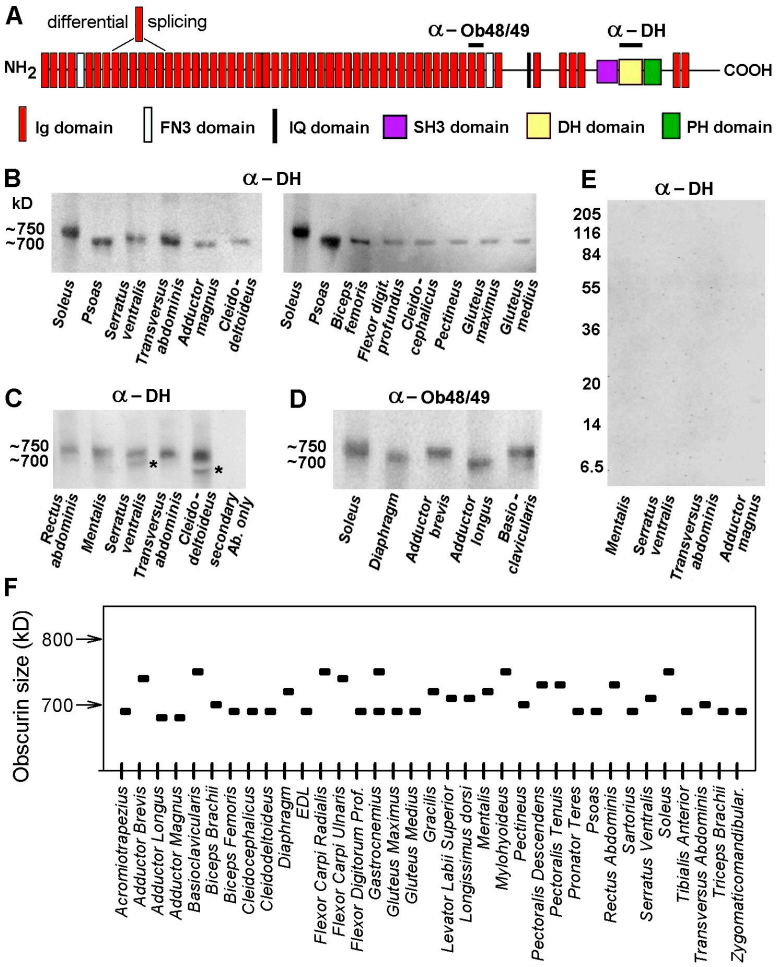


**Figure 11.** Size diversity of obscurin. (A) Domain structure of obscurin according to Young et al. (2001). Binding sites of the antibodies used in this study are indicated. (B–D) Western blots from 2% SDS-PAGE using (B and C) α-obscurin DH domain antibodies (asterisks in C, obscurin degradation bands) or (D) α-obscurin 48/49 antibodies. (E) Western blots from 12.5% polyacrylamide gels using α-obscurin DH domain antibodies. No signal was detectable in the $M_w$ range 6–250 kD. (F) Estimated molecular weight of obscurin isoforms for 35 different rabbit muscles.

meric (particularly collagen) and myofibrillar (titin) elements contribute substantially to total passive stiffness; the actual magnitude derived from one or the other source varies in a muscle-specific manner. As an example, rabbit soleus generated up to twice as much total PT as psoas, particularly at longer SLs (Fig. 8, A and B, solid curves), but psoas contains much stiffer titin than soleus (Fig. 8 F). In conclusion, some muscles have low titin-borne stiffness but high total passive stiffness, whereas the opposite is true for other muscles.

### Passive Stiffness and Fiber/MHC Composition

Using the results shown in Fig. 8 (A–E), we also correlated total, titin-based, and extramyofibrillar passive stiffness with the fiber/MHC composition (Fig. 8 F). Linear regression analysis revealed a statistically significant relationship between titin-based stiffness and the type-I fiber/MHC-I percentages ($R = -0.88$; $P < 0.05$), as well as the type-IIB/D fiber proportion ($R = 0.98$; $P < 0.005$). (As the five muscles studied contained no MHC-IIB isoform [Table I], there was also a significant correlation between titin-based stiffness and the MHC-IIA/D percentage.) In contrast, no correlations with the muscle type were found for both total and extramyofibrillar passive stiffness ($P >> 0.05$ in regression analyses). Thus, titin-based stiffness tends to be higher the faster the muscle, but the magnitude of both extramyofibrillar and total passive stiffness may be independent of muscle type.

### Obscurin Isoforms Vary in Size in a Muscle Type–dependent Manner

Finally we investigated the size distribution of obscurin, a giant protein (Fig. 11 A) that associates with the sarcomere and is involved in myocyte assembly and signaling (Young et al., 2001). Obscurin is of similar size but at least 10 times less abundant compared with nebulin (Young et al., 2001). Therefore the protein was identified on Western blots prepared from 2.0% SDS-PAGE gels using two different anti-obscurin antibodies (Fig. 11, B–D). Both antibodies should detect all large obscurin isoforms, as the site of differential splicing in the obscurin sequence is upstream of the antibody binding sites (Fig. 11 A). The size variability was moderate in the 35 rabbit muscles studied, ranging from ~680 to 750 kD (Fig. 11, B–D and F). Except for the gastrocne-

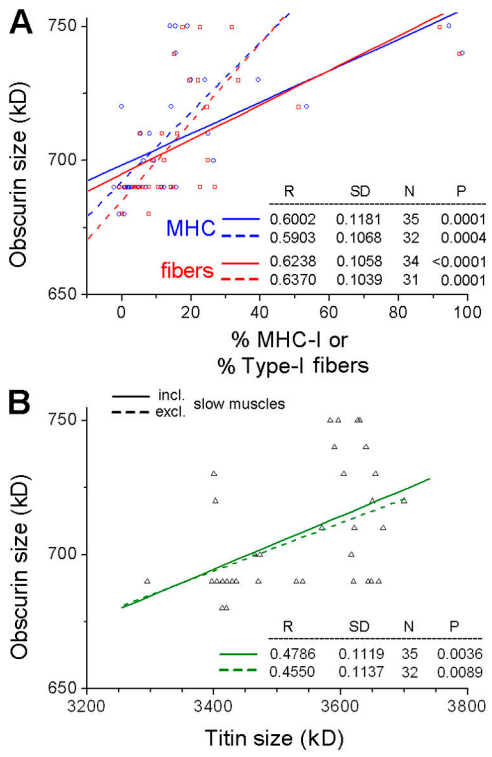


**Figure 12.** Relationships between obscurin size and (A) the proportions of type-I fibers (red squares and lines) or MHC-I isoform (blue circles and lines) and (B) titin size (major band) in 35 rabbit muscles. Linear regressions (results shown in lower right of each panel) are to all data points (solid lines), and after omitting points for the three slow muscles (dashed lines).

mius, which showed two bands of similar intensity on the blots, the muscles exhibited a clear major obscurin band. However, sometimes we detected a minor obscurin band of higher electrophoretic mobility compared with the major band (Fig. 11 C, asterisks). As the minor band was not consistently detectable even in a given muscle type (compare Fig. 11 B, left, with Fig. 11 C), we consider these signals to most likely represent degradation forms of obscurin (similar to the T2 bands of titin).

Small obscurin isoforms generated by differential splicing have been reported on the cDNA level in human muscles (Russell et al., 2002). Therefore we tested the set of rabbit skeletal muscles by Western blotting using 12.5% SDS-PAGE gels and α-DH antibody This antibody potentially detects the small isoforms, which have been reported to contain the DH domain. However, no obscurin isoforms were detectable in the molecular weight range between 6 and 250 kD (Fig. 11 E). Thus, the small isoforms may not be expressed in detectable amounts in rabbit muscles.

Given that obscurin may play a role for intermyofibrillar extensibility (Borisov et al., 2004), and thus, the mechanical properties of muscle, we studied the protein's size distribution in relation to the fiber/MHC proportions and titin isoform size (Fig. 12). The correlation with either the MHC-I isoform or the type-I fiber proportion was stronger than for titin (correlation coefficient, R ∼ 0.6; Fig. 12 A). As with titin, no significant relationships were found with any type-II fiber or MHC-II subtype (unpublished data). In contrast, the correlation between obscurin size and titin size (Fig. 12 B) was very modest (R = 0.45–0.48), indicating that there is only a trend for fibers with compliant (long) titin(s) to express large obscurin isoform.

## DISCUSSION

Although titin is the third most abundant protein in striated muscle cells (Maruyama et al., 1976; Wang et al., 1979), much less is known about the isoform diversity of this giant polypeptide than is the case for many of the contractile and regulatory proteins. This work investigated three previously unresolved issues: (1) the range of titin isoform sizes expressed in a large set of adult skeletal muscles; (2) the correlation of titin isoform diversity with both titin-based PT development and titin's contribution to total passive muscle stiffness; and (3) the relationship between titin isoform size, titin-based stiffness, and fiber-type/MHC isoform composition.

We found that the size diversity of titin is large, ranging from 3.3 to 3.7 MD. Muscles expressing large titins have low PT at the single-fiber and myofibril levels, whereas muscles with relatively small titins have higher PT. The relationship between titin size and active contractile parameters was very modest, suggesting a trend for predominantly slow fibers to express long titin isoforms. Consistent with this, titin-borne stiffness was lower the higher the proportion of slow fibers/MHC-I. In contrast, no significant correlations were found between titin size and the percentage of the various type-II fiber/MHC-II subtypes. Thus, besides fiber/MHC composition, other factors may determine the differential splicing of titin. We also showed that in whole muscles, a substantial contribution to total passive stiffness arises not only from titin but also from extramyofibrillar structures, particularly collagen. However, titin-based stiffness and total passive-muscle stiffness do not necessarily correlate; for instance, a muscle with low titin-based PT (e.g., soleus) can have greater total PT than a muscle with high titin-based PT (e.g., psoas). Because of the highly variable extramyofibrillar stiffness among muscles, the total passive stiffness does not depend on the muscle type. We conclude that the active and passive mechanical properties of skeletal muscles are not strongly correlated.

The idea that muscle type and titin size may be related had emerged, because the largest titin sequenced

to date occurs in human soleus, a muscle containing almost exclusively slow fibers, whereas a small titin was described in psoas, which has predominantly fast fibers (Freiburg et al., 2000). This work now suggests that the psoas is not a typical fast muscle in rabbit, as far as titin expression is concerned. Among the 34 predominantly fast muscles studied here (most rabbit skeletal muscles are fast-type), the psoas expresses the very shortest titin isoform (major, ~3.3 MD; minor, ~3.4 MD). However, in the other fast rabbit muscles, the titin size (major isoform) varied between 3.40 and 3.67 MD. Clearly, fast muscles containing predominantly type-II fibers/MHC-II can express either short or long titin(s). In contrast, slow muscles with a majority of type-I fibers/MHC-I only expressed long titin isoform(s). Among the 37 muscles studied only three were slow type. Soleus and diaphragm are well-known slow muscles and also the adductor brevis has previously been recognized as a predominantly slow muscle in rabbits (Hitomi et al., 2005). As the number of slow muscles in rabbit is apparently limited, it would be useful to study titin-size expression in larger vertebrate species containing a higher proportion of slow muscles, which are particularly needed to counterbalance gravity. We predict that skeletal titin sizes may tend to be greater in large species than in small rodents. It will be interesting to see whether our conclusion that predominantly slow muscles do not express short titin isoforms holds up in other species. Support for this conclusion comes from our observation that also the slower ones among the fast muscles express relatively long titin isoform(s).

We caution that the molecular masses of titin isoforms determined by 2% SDS-PAGE may differ somewhat from the true values, given that there are various factors that can affect the electrophoretic mobility of solubilized proteins, apart from molecular weight. But the mobility of titin bands of some muscles (human soleus, rabbit psoas, and major bands in rat and human heart) could be correlated with the isoform size determined by sequencing (Freiburg et al., 2000; Warren et al., 2004), thus providing useful markers. Importantly, differences in the electrophoretic mobility of titin isoforms could be detected with high confidence by comparing the positions of the titin band(s) of any muscle with those of the two bands for rabbit psoas titin on the same gel lane (Fig. 2). Considering the resolution limits of the gel detection system, we estimate that the titin sizes measured by us may be within <50 kD of the true sizes. Thus, the true titin isoform sizes in the 37 rabbit skeletal muscles could range between ~3,250 and 3,750 kD, but not beyond.

Ample evidence suggests that the titin isoform size is a main factor determining the PT level of a skeletal muscle fiber (Wang et al., 1991; Horowits, 1992) or myofibril (Linke et al., 1996). This notion was confirmed here by mechanical measurements on skinned single fibers and myofibrils; the PT level correlated inversely with titin size (Fig. 4 B). Myofibrils from the slow soleus (Fig. 5 B) and fibers from the predominantly slow diaphragm (Fig. 4 A) generated the lowest PT and it is likely that also other slow type muscles expressing large titin(s) have low PT. In a representative selection of five muscles with very different fiber/MHC compositions, titin-borne stiffness decreased with the percentage of type-I fibers/MHC-I isoforms (Fig. 8 F). As for the predominantly fast muscles, we found that even muscles with similar type-I fiber/MHC-I proportions (such as EDL and longissimus dorsi) can differ substantially in the magnitude of PT development (Fig. 4 A). Hence, this study establishes that titin-based PT depends somewhat on muscle type but is highly variable among the fast skeletal muscles.

What could be the reason slow muscles contain a low stiffness titin spring whereas fast muscles exhibit no preferred titin stiffness? A clue may come from the observation that titin elasticity is important for the positional stability of thick filaments during isometric contraction (Horowits and Podolsky, 1988). Then, a high stiffness titin spring would provide a higher stability than a low stiffness spring. A high stiffness spring may be required in very fast muscles generating the highest active tensions very rapidly. Indeed, most muscles with zero or very low content of type-I fibers/MHCs expressed short titin(s). This is the main reason why the relationship between titin size and type-I fiber/MHC percentage was clearly stronger when only the predominantly fast muscles were included in the analysis than when all muscles were included (Fig. 7, A and D). Why the modestly fast muscles (type-1 fiber/MHC-I content between ~5% and 20%) contain either stiff or compliant titin springs, remains a matter for future investigation. Slow muscles and the slower fast type muscles expressing long titins may not need a high positional stability of A bands for optimum performance.

Elegant work by Magid and Law (1985) in an earlier study on frog had suggested that myofibrils bear most of the resting tension of whole muscle, but our results on rabbit muscles do not support this view. Mechanical measurements of muscle strips before and after skinning, and following titin-specific proteolysis by low dose trypsin, demonstrated that extramyofibrillar elements contribute to total passive muscle stiffness on average no less than the titin filaments (Fig. 8). Along this line, various studies have shown that the extracellular matrix, especially the collagen content, isoform type, and collagen cross-linking status, is important for a muscle's in situ passive stiffness (Alnaqeeb et al., 1984; Kovanen et al., 1984a,b; Gosselin et al., 1998; Reich et al., 2000). In contrast, the contribution of intermediate filaments to PT (Ansved and Edström, 1991) appears to be very

small in the physiological SL range up to ~3.4 μm (Salviati et al., 1990; Wang et al., 1993). In our hands, the collagen network remained in rabbit psoas and soleus muscle strips after skinning and trypsin treatment (Fig. 10), and the residual PT following titin degradation was most likely due to these abundant collagen fibers.

The relative importance of titin versus extracellular (collagen, connective tissue) structures for the total PT level of whole muscle varied greatly between different muscle types (Fig. 8). Soleus muscle expressed a compliant titin isoform but contained a more extensive network of collagen fibers than psoas, which in turn expressed stiffer titin springs. However, the total passive stiffness of soleus exceeded that of psoas. Our data are consistent with a recent study on rabbits (Ducomps et al., 2003) showing that a glycolytic muscle like the psoas contains far less collagen than a pure oxidative (slow) muscle like the semimembranosus proprius. Also for rat, it has long been known that soleus contains abundant collagen fibers, making this muscle stiffer than the psoas (Kovanen et al., 1984a,b). This notwithstanding, the collagen content of other fast muscles may be higher than that of psoas. Indeed, the fast rabbit EDL and rectus femoris muscles were shown to contain more collagen than the slow semimembranosus proprius, and the collagen content scaled positively with total passive stiffness (Ducomps et al., 2003). Similarly, we found that the predominantly slow rabbit diaphragm exhibits low extramyofibrillar passive stiffness, whereas the predominantly fast EDL and gastrocnemius have relatively high extramyofibrillar stiffness (Fig. 8 F). There is no obvious correlation between extramyofibrillar passive stiffness and muscle type. Thus, the relative contribution of the extracellular matrix to total passive stiffness is unrelated to the active contractile characteristics.

Evidence has suggested that under unloading conditions or after intense exercise, skeletal muscles exhibit changes in passive elasticity (Kasper and Xun, 2000; Reich et al., 2000; Toursel et al., 2002; Goto et al., 2003), which may in part be caused by titin modifications. Accumulation of the T2 degradation form of titin takes place in the hindlimb muscles of rats and humans after eccentric exercise or power training (Yamaguchi et al., 1985; Trappe et al., 2002; McBride et al., 2003), although such changes have not always been reported (McGuigan et al., 2003; Kyrolainen et al., 2005). In cases where titin was found to be altered, the changes were explained by decreased titin expression or increased titin degradation, rather than by modification of titin isoform size. However, considering the resolution limits for titin size detection by SDS-PAGE, one cannot discount the possibility that titin isoform alterations nevertheless contribute to the observed stiffness changes. For instance, a switch toward smaller titin size(s) could add to the global stiffness changes caused by accumulation of connective tissue following immobilization, passive stretch, muscle activation, or exercise (Williams et al., 1988; Gosselin et al., 1998; Gajdosik, 2001; Ducomps et al., 2003). Then, pathological or physiological stimuli would alter the relative contributions of titin and the extracellular matrix to total passive stiffness (Reich et al., 2000; Neagoe et al., 2003). The large size variability of skeletal titins described in this study implies a potential for titin size alterations in health and disease, which may affect passive muscle stiffness.

Two other giant proteins in skeletal muscles, nebulin and obscurin, revealed much less size differences than titin did. The size of nebulin was similar (~700 kD) among all predominantly fast rabbit muscles, but substantially increased in the three slow muscles (Fig. 3 C). Nebulin size was shown to correlate with the thin filament length in skeletal muscles of different species (Kruger et al., 1991), and a role for nebulin as a ruler of the thin filament length has been suggested (Kruger et al., 1991; Labeit et al., 1991; Pfuhl et al., 1994) and confirmed recently (McElhinny et al., 2005). Our results thus raise the possibility that slow muscles contain longer thin filaments than fast muscles, an issue that requires further study.

Obscurin belongs to the intracellular Ig domain superfamily and associates with sarcomeres in the M line region (Young et al., 2001; Borisov et al., 2004). The isoform size of cardiac obscurin is modified in heart development and disease (Opitz et al., 2004; Makarenko et al., 2004) and one could speculate that obscurin size changes also during maturation of a given skeletal muscle. Here we showed by Western blotting that obscurin varies in size among normal adult rabbit skeletal muscles by up to ~70 kD (680–750 kD). This size difference appears to correlate well with the differential splicing of six immunoglobulin domains near obscurin's $NH_2$ terminus (Young et al., 2001). Since obscurin is involved in the lateral connection of M bands to the sarcolemma (Bagnato et al., 2003) and could also provide an elastic link between adjacent myofibrils (Borisov et al., 2004), the protein may have a passive mechanical role, like titin, but in the muscle's transverse direction. However, the correlation between obscurin size and titin size (and hence, titin-based PT) was low (Fig. 12 B). Interestingly, a much stronger correlation was found between obscurin size and the percentage of type-I fibers/MHC-I isoforms (Fig. 12 A). Thus, slow muscles tend to express a large obscurin isoform, fast muscles a small isoform.

In summary, this study of a set of 37 adult rabbit skeletal muscles allows the following conclusions. (a) Titin isoform size varies between ~3.3 and 3.7 MD in differ-

ent muscles; most muscles express a single titin isoform, a few muscles two isoforms. (b) Large titin isoform(s) give rise to low PT of the myofibrils/fibers, smaller titin(s) to higher PT. (c) High titin-based PT not necessarily implies high total passive stiffness of a muscle, which is greatly determined also by extramyofibrillar structures, particularly collagen. (d) The relative importance of titin and the extracellular matrix for total passive stiffness can be very different in different muscles. (e) Titin size is modestly correlated with the proportion of type-I fibers/MHC-I, but not with that of the various type-II fibers/MHC-II subtypes. (f) Slow rabbit muscles express long titin isoform(s), whereas predominantly fast muscles can express shorter or longer titin(s). (g) Thus, slow muscles have low titin-based PT but this tension is highly variable in fast muscles. (h) Titin-based stiffness, but not extramyofibrillar passive stiffness, correlates with the muscle type. (i) Two other giant proteins, nebulin and obscurin, varied in size by up to ~70 kD in a muscle type–dependent manner, suggesting that slow muscles usually express a larger isoform of nebulin and obscurin than predominantly fast muscles.

We thank Anita Kühner for expert technical assistance on histochemistry, Rita Hassenrück for help with myosin typing and electron microscopy, and Lars-Henrik Meyer for running a titin gel.

We acknowledge financial support of the Deutsche Forschungsgemeinschaft (Li 690/6-2; SFB 629 "Molecular Cell Dynamics").

Olaf S. Andersen served as editor.

Submitted: 13 July 2005
Accepted: 26 September 2005

## REFERENCES

Agarkova, I., R. Schoenauer, E. Ehler, L. Carlsson, E. Carlsson, L.E. Thornell, and J.C. Perriard. 2004. The molecular composition of the sarcomeric M-band correlates with muscle fiber type. *Eur. J. Cell Biol.* 83:193–204.

Aigner, S., B. Gohlsch, N. Hamalainen, R.S. Staron, A. Uber, U. Wehrle, and D. Pette. 1993. Fast myosin heavy chain diversity in skeletal muscles of the rabbit: heavy chain IId, not IIb predominates. *Eur. J. Biochem.* 211:367–372.

Alnaqeeb, M.A., N.S. Zaid, and G. Goldspink. 1984. Connective tissue changes and physical properties of developing and ageing skeletal muscle. *J. Anat.* 139:677–689.

Andruchov, O., Y. Wang, O. Andruchova, and S. Galler. 2004. Functional properties of skinned rabbit skeletal and cardiac muscle preparations containing α-cardiac myosin heavy chain. *Pflugers Arch.* 448:44–53.

Ansved, T., and L. Edström. 1991. Effects of age on fibre structure, ultrastructure and expression of desmin and spectrin in fast- and slow-twitch rat muscles. *J. Anat.* 174:61–79.

Bagnato, P., V. Barone, E. Giacomello, D. Rossi, and V. Sorrentino. 2003. Binding of an ankyrin-1 isoform to obscurin suggests a molecular link between the sarcoplasmic reticulum and myofibrils in striated muscles. *J. Cell Biol.* 160:245–253.

Bagni, M.A., G. Cecchi, B. Colombini, and F. Colomo. 2002. A non-cross-bridge stiffness in activated frog muscle fibers. *Biophys. J.* 82: 3118–3127.

Borisov, A.B., A. Kontrogianni-Konstantopoulos, R.J. Bloch, M.V. Westfall, and M.W. Russell. 2004. Dynamics of obscurin localization during differentiation and remodeling of cardiac myocytes: obscurin as an integrator of myofibrillar structure. *J. Histochem. Cytochem.* 52:1117–1127.

Capdevila, X., S. Lopez, N. Bernard, E. Rabischong, M. Ramonatxo, G. Martinazzo, and C. Prefaut. 2003. Effects of controlled mechanical ventilation on respiratory muscle contractile properties in rabbits. *Intensive Care Med.* 29:103–110.

Ducomps, C., P. Mauriège, B. Darche, S. Combes, F. Lebas, and J.P. Doutreloux. 2003. Effects of jump training on passive mechanical stress and stiffness in rabbit skeletal muscle: role of collagen. *Acta Physiol. Scand.* 178:215–224.

Freiburg, A., K. Trombitas, W. Hell, O. Cazorla, F. Fougerousse, T. Centner, B. Kolmerer, C. Witt, J.S. Beckmann, C.C. Gregorio, et al. 2000. Series of exon-skipping events in the elastic spring region of titin as the structural basis for myofibrillar elastic diversity. *Circ. Res.* 86:1114–1121.

Frey, M., P. Giovanoli, and C. Meuli-Simmen. 1998. The qualification of different free muscle transplants to reconstruct mimic function: an experimental study in rabbits. *Plast. Reconstr. Surg.* 101:1774–1783.

Friden, J., and R.L. Lieber. 2003. Spastic muscle cells are shorter and stiffer than normal cells. *Muscle Nerve.* 27:157–164.

Fryer, M.W., P.W. Gage, I.R. Neering, A.F. Dulhunty, and G.D. Lamb. 1988. Paralysis of skeletal muscle by butanedione monoxime, a chemical phosphatase. *Pflugers Arch.* 411:76–79.

Fuentes, I., A.R. Cobos, and L.A. Segade. 1998. Muscle fibre types and their distribution in the biceps and triceps brachii of the rat and rabbit. *J. Anat.* 192:203–210.

Funatsu, T., H. Higuchi, and S. Ishiwata. 1990. Elastic filaments in skeletal muscle revealed by selective removal of thin filaments with plasma gelsolin. *J. Cell Biol.* 110:53–62.

Gajdosik, R.L. 2001. Passive extensibility of skeletal muscle: review of the literature with clinical implications. *Clin. Biomech. (Bristol, Avon).* 16:87–101.

Gondret, F., L. Lefaucheur, A. D'Albis, and M. Bonneau. 1996. Myosin isoform transitions in four rabbit muscles during postnatal growth. *J. Muscle Res. Cell Motil.* 17:657–667.

Gosselin, L.E., C. Adams, T.A. Cotter, R.J. McCormick, and D.P. Thomas. 1998. Effect of exercise training on passive stiffness in locomotor skeletal muscle: role of extracellular matrix. *J. Appl. Physiol.* 85:1011–1016.

Goto, K., R. Okuyama, M. Honda, H. Uchida, T. Akema, Y. Ohira, and T. Yoshioka. 2003. Profiles of connectin (titin) in atrophied soleus muscle induced by unloading of rats. *J. Appl. Physiol.* 94: 897–902.

Granzier, H.L., and S. Labeit. 2004. The giant protein titin: a major player in myocardial mechanics, signaling, and disease. *Circ. Res.* 94:284–295.

Granzier, H., M. Helmes, O. Cazorla, M. McNabb, D. Labeit, Y. Wu, R. Yamasaki, A. Redkar, M. Kellermayer, S. Labeit, and K. Trombitas. 2000. Mechanical properties of titin isoforms. *Adv. Exp. Med. Biol.* 481:283–300.

Hamalainen, N., and D. Pette. 1993. The histochemical profiles of fast fiber types IIB, IID, and IIA in skeletal muscles of mouse, rat, and rabbit. *J. Histochem. Cytochem.* 41:733–743.

Helmes, M., C.C. Lim, R. Liao, A. Bharti, L. Cui, and S.B. Sawyer. 2003. Titin determines the Frank-Starling relation in early diastole. *J. Gen. Physiol.* 121:97–110.

Higuchi, H. 1992. Changes in contractile properties with selective digestion of connectin (titin) in skinned fibers of frog skeletal muscle. *J. Biochem. (Tokyo).* 111:291–295.

Hitomi, Y., T. Kizaki, S. Watanabe, G. Matsumura, Y. Fujioka, S. Haga, T. Izawa, N. Taniguchi, and H. Ohno. 2005. Seven skeletal muscles rich in slow muscle fibers may function to sustain neutral position in the rodent hindlimb. *Comp. Biochem. Physiol. B Biochem. Mol. Biol.* 140:45–50.

Horowits, R. 1992. Passive force generation and titin isoforms in mammalian skeletal muscle. *Biophys. J.* 61:392–398.

Horowits, R., and R.J. Podolsky. 1988. Thick filament movement and isometric tension in activated skeletal muscle. *Biophys. J.* 54: 165–171.

Horowits, R., E.S. Kempner, M.E. Bisher, and R.J. Podolsky. 1986. A physiological role for titin and nebulin in skeletal muscle. *Nature.* 323:160–164.

Jimenez-Fuentes, M.A., J. Gea, M. Marinan, J.B. Galdiz, F. Gallego, and J.M. Broquetas. 1998. Cellular homogeneity in diverse portions of the diaphragm. *Arch. Bronconeumol.* 34:82–86.

Joosten, H.F., P. Wirtz, H.O. Verbeek, and A. Hoekstra. 1981. Splayleg: a spontaneous limb defect in rabbits. Genetics, gross anatomy, and microscopy. *Teratology.* 24:87–104.

Kasper, C.E., and L. Xun. 2000. Expression of titin in skeletal muscle varies with hind-limb unloading. *Biol. Res. Nurs.* 2:107–115.

Kellermayer, M.S., S.B. Smith, H.L. Granzier, and C. Bustamante. 1997. Folding-unfolding transitions in single titin molecules characterized with laser tweezers. *Science.* 276:1112–1116.

Kovanen, V., H. Suominen, and E. Heikkinen. 1984a. Mechanical properties of fast and slow skeletal muscle with special reference to collagen and endurance training. *J. Biomech.* 17:725–735.

Kovanen, V., H. Suominen, and E. Heikkinen. 1984b. Collagen of slow twitch and fast twitch muscle fibres in different types of rat skeletal muscle. *Eur. J. Appl. Physiol. Occup. Physiol.* 52:235–242.

Kruger, M., J. Wright, and K. Wang. 1991. Nebulin as a length regulator of thin filaments of vertebrate skeletal muscles: correlation of thin filament length, nebulin size, and epitope profile. *J. Cell Biol.* 115:97–107.

Kulke, M., C. Neagoe, B. Kolmerer, A. Minajeva, H. Hinssen, B. Bullard, and W.A. Linke. 2001. Kettin, a major source of myofibrillar stiffness in *Drosophila* indirect flight muscle. *J. Cell Biol.* 154:1045–1057.

Kyrolainen, H., J. Avela, J.M. McBride, S. Koskinen, J.L. Andersen, S. Sipila, T.E. Takala, and P.V. Komi. 2005. Effects of power training on muscle structure and neuromuscular performance. *Scand. J. Med. Sci. Sports.* 15:58–64.

Labeit, S., and B. Kolmerer. 1995. Titins, giant proteins in charge of muscle ultrastructure and elasticity. *Science.* 270:293–296.

Labeit, S., T. Gibson, A. Lakey, K. Leonard, M. Zeviani, P. Knight, J. Wardale, and J. Trinick. 1991. Evidence that nebulin is a protein-ruler in muscle thin filaments. *FEBS Lett.* 282:313–316.

Le Souef, P.N., S.J. England, H.A. Stogryn, and A.C. Bryan. 1988. Comparison of diaphragmatic fatigue in newborn and older rabbits. *J. Appl. Physiol.* 65:1040–1044.

Lexell, J., J.C. Jarvis, J. Currie, D.Y. Downham, and S. Salmons. 1994. Fibre type composition of rabbit tibialis anterior and extensor digitorum longus muscles. *J. Anat.* 185:95–101.

Li, H., W.A. Linke, A.F. Oberhauser, M. Carrion-Vazquez, J.G. Kerkvliet, H. Lu, P.E. Marszalek, and J.M. Fernandez. 2002. Reverse engineering of the giant muscle protein titin. *Nature.* 418: 998–1002.

Lind, A., and D. Kernell. 1991. Myofibrillar ATPase histochemistry of rat's skeletal muscles: a "two-dimensional" quantitative approach. *J. Histochem. Cytochem.* 39:589–597.

Linke, W.A., M. Ivemeyer, S. Labeit, H. Hinssen, J.C. Rüegg, and M. Gautel. 1997. Actin-titin interaction in cardiac myofibrils: probing a physiological role. *Biophys. J.* 73:905–919.

Linke, W.A., M. Ivemeyer, P. Mundel, M.R. Stockmeier, and B. Kolmerer. 1998. Nature of PEVK-titin elasticity in skeletal muscle. *Proc. Natl. Acad. Sci. USA.* 95:8052–8057.

Linke, W.A., M. Ivemeyer, N. Olivieri, B. Kolmerer, J.C. Rüegg, and S. Labeit. 1996. Towards a molecular understanding of the elasticity of titin. *J. Mol. Biol.* 261:62–71.

Linke, W.A., V.I. Popov, and G.H. Pollack. 1994. Passive and active tension in single cardiac myofibrils. *Biophys. J.* 67:782–792.

Linke, W.A., and M.C. Leake. 2004. Multiple sources of passive stress relaxation in muscle fibers. *Phys. Med. Biol.* 49:3613–3627.

Lobley, G.E., A.B. Wilson, and A.S. Bruce. 1977. An estimation of the fibre type composition of eleven skeletal muscles from New Zealand white rabbits between weaning and early maturity. *J. Anat.* 123:501–513.

Lutz, H., M. Ermini, E. Jenny, and F. Joris. 1978. The influence of aging on the myosin type of the rabbit soleus and longissimus dorsi muscles. *Aktuelle Gerontol.* 8:667–673.

Mabuchi, K., D. Szvetko, K. Pinter, and F.A. Sreter. 1982. Type IIB to IIA fiber transformation in intermittently stimulated rabbit muscles. *Am. J. Physiol.* 242:C373–C381.

MacArthur, D.G., and K.N. North. 2004. A gene for speed? The evolution and function of α-actinin-3. *Bioessays.* 26:786–795.

Magid, A., and D.J. Law. 1985. Myofibrils bear most of the resting tension in frog skeletal muscle. *Science.* 230:1280–1282.

Makarenko, I., C.A. Opitz, M.C. Leake, C. Neagoe, M. Kulke, J.K. Gwathmey, F. del Monte, R.J. Hajjar, and W.A. Linke. 2004. Passive stiffness changes caused by upregulation of compliant titin isoforms in human DCM hearts. *Circ. Res.* 95:708–716.

Marko, J.F., and E.D. Siggia. 1995. Stretching DNA. *Macromolecules.* 28:8759–8770.

Maruyama, K., R. Natori, and Y. Nonomura. 1976. New elastic protein from muscle. *Nature.* 262:58–60.

Maruyama, K., H. Sawada, S. Kimura, K. Ohashi, H. Higuchi, and Y. Umazume. 1984. Connectin filaments in stretched skinned fibers of frog skeletal muscle. *J. Cell Biol.* 99:1391–1397.

McBride, J.M., T. Triplett-McBride, A.J. Davie, P.J. Abernethy, and R.U. Newton. 2003. Characteristics of titin in strength and power athletes. *Eur. J. Appl. Physiol.* 88:553–557.

McElhinny, A.S., C. Schwach, M. Valichnac, S. Mount-Patrick, and C.C. Gregorio. 2005. Nebulin regulates the assembly and lengths of the thin filaments in striated muscle. *J. Cell Biol.* 170:947–957.

McGuigan, M.R., M.J. Sharman, R.U. Newton, A.J. Davie, A.J. Murphy, and J.M. McBride. 2003. Effect of explosive resistance training on titin and myosin heavy chain isoforms in trained subjects. *J. Strength Cond. Res.* 17:645–651.

Miller, M.K., H. Granzier, E. Ehler, and C.C. Gregorio. 2004. The sensitive giant: the role of titin-based stretch sensing complexes in the heart. *Trends Cell Biol.* 14:119–126.

Minajeva, A., M. Kulke, J.M. Fernandez, and W.A. Linke. 2001. Unfolding of titin domains explains the viscoelastic behavior of skeletal myofibrils. *Biophys. J.* 80:1442–1451.

Minajeva, A., C. Neagoe, M. Kulke, and W.A. Linke. 2002. Titin-based contribution to shortening velocity of rabbit skeletal myofibrils. *J. Physiol.* 540.1:177-188.

Mutungi, G., and K.W. Ranatunga. 1996. The viscous, viscoelastic and elastic characteristics of resting fast and slow mammalian (rat) muscle fibres. *J. Physiol.* 496:827–836.

Neagoe, C., M. Kulke, F. del Monte, J.K. Gwathmey, P.P. de Tombe, R.J. Hajjar, and W.A. Linke. 2002. Titin isoform switch in ischemic human heart disease. *Circulation.* 106:1333–1341.

Neagoe, C., C.A. Opitz, I. Makarenko, and W.A. Linke. 2003. Gigantic variety: expression patterns of titin isoforms in striated muscles and consequences for myofibrillar passive stiffness. *J. Muscle Res. Cell Motil.* 24:175–189.

O'Connell, B., L.T. Nguyen, and G.M. Stephenson. 2004. A single-fibre study of the relationship between MHC and TnC isoform composition in rat skeletal muscle. *Biochem. J.* 378:269–274.

Opitz, C.A., M. Kulke, M.C. Leake, C. Neagoe, H. Hinssen, R.J. Hajjar, and W.A. Linke. 2003. Damped elastic recoil of the titin spring in myofibrils of human myocardium. *Proc. Natl. Acad. Sci. USA*. 100:12688–12693.

Opitz, C.A., M.C. Leake, I. Makarenko, V. Benes, and W.A. Linke. 2004. Developmentally regulated switching of titin size alters myofibrillar stiffness in the perinatal heart. *Circ. Res.* 94:967–975.

Pagliassotti, M.J., and C.M. Donovan. 1990. Influence of cell heterogeneity on skeletal muscle lactate kinetics. *Am. J. Physiol.* 258: E625–E634.

Pfuhl, M., S.J. Winder, and A. Pastore. 1994. Nebulin, a helical actin binding protein. *EMBO J.* 13:1782–1789.

Popesko, P., V. Rajtova, and J. Horak. 1992. A Colour Atlas of the Anatomy of Small Laboratory Animals. Volume 1: Rabbit, Guinea Pig. Wolfe Publishing, London. 256 pp.

Rab, M., C. Neumayer, R. Koller, L.P. Kamolz, W. Haslik, R. Gassner, P. Giovanoli, G. Schaden, and M. Frey. 2000. Histomorphology of rabbit thigh muscles: establishment of standard control values. *J. Anat.* 196:203–209.

Ranatunga, K.W., and P.E. Thomas. 1990. Correlation between shortening velocity, force-velocity relation and histochemical fibre-type composition in rat muscles. *J. Muscle Res. Cell Motil.* 11: 240–250.

Reich, T.E., S.L. Lindstedt, P.C. LaStayo, and D.J. Pierotti. 2000. Is the spring quality of muscle plastic? *Am. J. Physiol. Regul. Integr. Comp. Physiol.* 278:R1661–R1666.

Rief, M., M. Gautel, F. Oesterhelt, J.M. Fernandez, and H.E. Gaub. 1997. Reversible unfolding of individual titin immunoglobulin domains by AFM. *Science.* 276:1109–1112.

Rouanet, P., and F. Bacou. 1993. Changes in fibre type, metabolic character and acetylcholinesterase forms in rabbit skeletal muscle following stretch and electrical stimulation. *Neuromuscul. Disord.* 3:401–405.

Russell, M.W., M.O. Raeker, K.A. Korytkowski, and K.J. Sonneman. 2002. Identification, tissue expression and chromosomal localization of human obscurin-MLCK, a member of the titin and Dbl families of myosin light chain kinases. *Gene.* 282:237–246.

Salviati, G., R. Betto, and D. Danieli Betto. 1982. Polymorphism of myofibrillar proteins of rabbit skeletal-muscle fibres. An electrophoretic study of single fibres. *Biochem. J.* 207:261–272.

Salviati, G., R. Betto, S. Ceoldo, and S. Pierobon-Bormioli. 1990. Morphological and functional characterization of the endosarcomeric elastic filament. *Am. J. Physiol.* 259:C144–C149.

Schiaffino, S., and C. Reggiani. 1994. Myosin isoforms in mammalian skeletal muscle. *J. Appl. Physiol.* 77:493–501.

Sorimachi, H., A. Freiburg, B. Kolmerer, S. Ishiura, G. Stier, C.C. Gregorio, D. Labeit, W.A. Linke, K. Suzuki, and S. Labeit. 1997. Tissue-specific expression and α-actinin binding properties of the Z-disc titin: implications for the nature of vertebrate Z-discs. *J. Mol. Biol.* 270:688–695.

Staron, R.S., and D. Pette. 1986. Correlation between myofibrillar ATPase activity and myosin heavy chain composition in rabbit muscle fibers. *Histochemistry.* 86:19–23.

Talmadge, R.J., and R.R. Roy. 1993. Electrophoretic separation of rat skeletal muscle myosin heavy-chain isoforms. *J. Appl. Physiol.* 75:2337–2340.

Termin, A., R.S. Staron, and D. Pette. 1989. Myosin heavy chain isoforms in histochemically defined fiber types of rat muscle. *Histochemistry.* 92:453–457.

Thomason, D.B., K.M. Baldwin, and R.E. Herrick. 1986. Myosin isozyme distribution in rodent hindlimb skeletal muscle. *J. Appl. Physiol.* 60:1923–1931.

Tikunov, B.A., H.L. Sweeney, and L.C. Rome. 2001. Quantitative electrophoretic analysis of myosin heavy chains in single muscle fibers. *J. Appl. Physiol.* 90:1927–1935.

Toursel, T., L. Stevens, H. Granzier, and Y. Mounier. 2002. Passive tension of rat skeletal soleus muscle fibers: effects of unloading conditions. *J. Appl. Physiol.* 92:1465–1472.

Trappe, T.A., J.A. Carrithers, F. White, C.P. Lambert, W.J. Evans, and R.A. Dennis. 2002. Titin and nebulin content in human skeletal muscle following eccentric resistance exercise. *Muscle Nerve.* 25:289–292.

Trombitas, K., M. Greaser, S. Labeit, J.P. Jin, M. Kellermayer, M. Helmes, and H. Granzier. 1998. Titin extensibility in situ: entropic elasticity of permanently folded and permanently unfolded molecular segments. *J. Cell Biol.* 140:853–859.

Tskhovrebova, L., and J. Trinick. 2004. Properties of titin immunoglobulin and fibronectin-3 domains. *J. Biol. Chem.* 279:46351–46354.

Vigneron, P., F. Bacou, and C.R. Ashmore. 1976. Distribution heterogeneity of muscle fiber types in the rabbit longissimus muscle. *J. Anim. Sci.* 43:985–988.

Wade, R., R. Eddy, T.B. Shows, and L. Kedes. 1990. cDNA sequence, tissue-specific expression, and chromosomal mapping of the human slow-twitch skeletal muscle isoform of troponin I. *Genomics.* 7:346–357.

Wang, K., R. McCarter, J. Wright, J. Beverly, and R. Ramirez-Mitchell. 1991. Regulation of skeletal muscle stiffness and elasticity by titin isoforms: a test of the segmental extension model of resting tension. *Proc. Natl. Acad. Sci. USA.* 88:7101–7105.

Wang, K., R. McCarter, R. Wright, J. Beverly, and R. Ramirez-Mitchell. 1993. Viscoelasticity of the sarcomere matrix of skeletal muscles. The titin-myosin composite filament is a dual-stage molecular spring. *Biophys. J.* 64:1161–1177.

Wang, K., J. McClure, and A. Tu. 1979. Titin: major myofibrillar component of striated muscle. *Proc. Natl. Acad. Sci. USA.* 76: 3698–3702.

Wang, L.C., and D. Kernell. 2001. Fibre type regionalisation in lower hindlimb muscles of rabbit, rat and mouse: a comparative study. *J. Anat.* 199:631–643.

Warren, C.M., P.R. Krzesinski, K.S. Campbell, R.L. Moss, and M.L. Greaser. 2004. Titin isoform changes in rat myocardium during development. *Mech. Dev.* 121:1301–1312.

Williams, P.E., T. Catanese, E.G. Lucey, and G. Goldspink. 1988. The importance of stretch and contractile activity in the prevention of connective tissue accumulation in muscle. *J. Anat.* 158: 109–114.

Wingerd, B.D. 1985. Rabbit Dissection Manual. Johns Hopkins University Press, Baltimore, MD. 80 pp.

Yamaguchi, M., Y. Nakayama, and J. Nishikawa. 1985. Studies on exercise and an elastic protein "connectin" in hindlimb muscle of growing rat. *Jpn. J. Physiol.* 35:21–32.

Yamazaki, H., M. Abe, and K. Kanbara. 2003. Changes of fiber type ratio and diameter in rabbit skeletal muscle during limb lengthening. *J. Orthop. Sci.* 8:75–78.

Young, P., E. Ehler, and M. Gautel. 2001. Obscurin, a giant sarcomeric Rho guanine nucleotide exchange factor protein involved in sarcomere assembly. *J. Cell Biol.* 154:123–136.